Graph matching as a means to energy-visualisation of a counter-flow heat exchanger

S van Graan

22711775

Dissertation submitted in partial fulfilment of the requirements for the degree Master of Engineering in Computer and Electronic Engineering at the Potchefstroom Campus of the North-West University

Supervisor: Prof G van Schoor

Co-supervisor: Prof K Uren

May 2017

"So let us come boldly to the throne of our gracious God. There we will receive his mercy, and we will find grace to help us when we need it most." Hebrews 4:16

Abstract

The objective of this study is to develop an energy visualisation of a counter-flow heat exchanger by making use of graph matching. The energy visualisation developed should be suitable for the purpose of fault diagnosis. Since energy is a multi-domain parameter, it is considered as an ideal approach for fault diagnosis.

The heat exchanger model used in this study is based on the gas cooler of an operating CO_2 heat pump test bench at the North-West University. A simplified model is developed in Flownex®; a simulation environment that can be used to simulate flow and heat transfer systems. Experimental data have been used to validate the components available in Flownex®. The model is adjusted to incorporate faults by adding the necessary Flownex® components. The faults concerned include a fluid leak, heat leakage and fouling.

Energy can be seen as a unifying concept convenient to address multi-domain systems. System information can be reduced to the essentials if energy is used as modelling parameter. The concepts of exergy and energy flow rate are used to fully represent the energy of the heat exchanger. Energy information is related to attributed linear graphs and graph matching is applied on these graphs. The resulting outputs include a permutation matrix, a cost matrix and a distance parameter. Graph matching is a technique that describes how similar two graphs are. Therefore, the three outputs can be viewed as a description of how similar the energy information contained in two graphs are.

Visualisation is achieved by computing and plotting the eigenvalues of the cost matrix. Using this visual presentation, a procedure to identify which of the three faults has occurred, is developed. The procedure is successful in identifying a fluid leak, heat leakage and fouling.

This study confirms that the energy visualisation of a counter-flow heat exchanger can be achieved by making use of graph matching. The use of energy reduces the number of parameters considered and makes it possible to treat the fluid and thermal domains found in a heat exchanger in a similar fashion. This study shows that energy visualisation and graph matching are suitable for the purpose of fault diagnosis in a practical system.

Keywords: *graph matching, energy visualisation, counter-flow heat exchanger, fault diagnosis*

Acknowledgements

To my dear Lord and Father, thank you for your blessings and allowing me to pursue one of my dreams. Thank you for the grace and strength you bestowed upon me during this study.

To my study leaders, Prof George and Prof Kenny, thank you for your belief in me and all the hard work you had to put in for the completion of this study. Thank you for being my mentors in academics as well as in living your daily life as a Christian and all the compassion that entails. Your special way of doing things and your dry humour is appreciated.

Mamma and Pappa (Esmé and Johan van Graan), thank you for always being there for me and supporting me in every decision. Without you, none of this would have been possible. Thank you for never doubting my abilities and praising my successes.

Jomé, Ilse, Laura, Germari, Soemie and Dalene, thank you for being there when I needed to talk. Thank you for drying my tears on numerous occasions and telling me that everything will be okay.

Thank you to all my friends and family for your prayers and support.

A special thanks is also extended to M-Tech Industrial (Pty) Ltd and THRIP for funding this research. Thank you M-Tech Industrial (Pty) LTd for the access to Flownex® simulation software.

Contents

List of Figures

List of Tables

Nomenclature

List of Symbols

A	Area
$\mathbf{C}$	Cost Matrix
D	Distance parameter
h	Specific enthalpy
l	Length
$\dot{m}$	Mass flow rate
M	Matching operator
M	Main grid point
$\mathbf{N}$	Node signature matrix
P	Pressure
$\mathbf{P}$	Permutation matrix
$\dot{q}$	Energy flow rate
s	Specific entropy
S	Secondary grid point
T	Temperature
U	Heat transfer coefficient
x	Specific exergy

List of Subscripts

c	Cold side
F	Comparison/Fault matrix
h	Hot side
in	Inlet
out	Outlet
O	Original matrix
w	Wall
0	Reference state

Chapter 1

Introduction

This chapter starts with a background on energy as a quantity of system characterisation and motivates the use of a heat exchanger as a case study. The concept of a reference signature is discussed. The focus then turns to graph matching as a tool to achieve energy visualisation. Next, the issues to be addressed are discussed as well as the methodology involved. Lastly the chapter concludes with an outline of the rest of this document.

1.1 Background

Energy is required to sustain life and is essential to address basic human needs. In [1] the total final consumption by fuel of the world in 2014 was given as 9 425.69 Mega tons per oil equivalent (Mtoe). The largest fuel share sectors are 39.94% oil, 18.1% electricity and 15.1% natural gas. The demand for energy is ever increasing; the outlook for total final consumption by fuel for 2040 is given as 12 244 Mtoe.

The industry sector is one of the largest sectors to consume energy. In 2014 the industry sector accounted 29.2% of the total final consumption by fuel. This is expected to increase to 31.3% by 2040 [1]. There is a lot of focus on studying how energy can be generated and used more efficiently. This can only be done by looking closer at the energy flow of a system.

Energy is a very useful quantity to characterise any system or process. Energy is a universal concept that can be used for systems that transpire in more than one domain and can be understood by people that work in different disciplines of science and engineering [2]. Furthermore, the use of energy representation might lead to additional information regarding a system that is not present in the current way of modelling a system in terms of domain properties and by making use of fundamental equations.

A system that is widely used and forms an integral part of most large scale industrial processes is a heat exchanger. By decreasing the use of energy in heat exchangers, the total energy consumption can be decreased. A heat exchanger is a device that is used to transfer heat between two different fluids. The two fluids are kept apart and at different temperatures [3].

Heat exchangers are commonly used in chemical processes, power production as well as in HVAC (heating, ventilation and air conditioning) systems, both commercially and industrially. Configuration and direction flow are two categories typically used to classify heat exchangers [4]. The class of heat exchanger used depends on the application.

Fouling is a fault that occurs in heat exchangers and is described as a serious and ongoing issue that negatively impacts the efficiency of a heat exchanger [5]. Inadequate insulation and leaks in the heat exchanger pipes are other phenomena that affect the efficiency of a heat exchanger.

As heat exchangers are so widely used; if faults, like the above mentioned, can be correctly identified and corrected, it could lead to a significant decrease in unnecessary energy loss. In order to achieve this, some sort of energy signature will be needed. This energy signature should describe the faultless system. The signature generated will then be compared to the data of the system with a fault in order to identify the fault.

A graph theoretic approach is chosen as the framework to achieve the generation of the signature. The approach is called attributed graph matching and is used to describe graph similarities [6]. Graph matching enables the comparison of the energy signature and data with faults. Graph matching can only be applied to linear graphs. A linear graph is a graph in which vertices denote the nodes of the original system and the edges denote the energy flow by making use of through and across variables [7]. One of the functional features of linear graphs is that they can easily be converted to a matrix. A matrix is convenient to use in computer processing [8]. In an attributed linear graph, the nodes as well as the edges have labels. Labels

can be numeric or symbolic [6].

1.2 Problem Statement

The objective of this study is to apply a linear graph-based approach to visualise the energy in a counter flow heat exchanger. The visualisation must be sensitive to faults that can occur in a heat exchanger and must be able to identify the type of fault that has occurred. Energy, a multi-domain element, must be used as the modelling tool to incorporate both the fluid and thermal domains of a heat exchanger. The graph matching technique chosen is applied to the energy information of a double pipe counter-flow single phase heat exchanger with warm CO_2 as the working fluid which is used to heat water.

1.3 Issues to be addressed and methodology

In this section the most important aspects or challenges of the study are discussed as well as how they will be resolved.

1.3.1 Model of a heat exchanger

A model of a heat exchanger is needed in order characterise the heat exchanger in terms of energy. An existing Flownex® model of a double pipe counter flow single phase will be used. The model is based on the staggered grid approach. A model is used to simulate the heat exchanger with and without a fault. The faults that will be simulated include a heat leak, a fluid leak and fouling in the pipes.

1.3.2 Energy characterisation of a heat exchanger

Exergy and energy flow will be used to represent the energy in the heat exchanger. The aforementioned can be computed by making use of the parameters that are available in the Flownex® model as well as other thermodynamic properties that can be derived from the

parameters of the Flownex® model by making use of Engineering Equation Solver (EES is a software package used to solve engineering equations and can compute the thermodynamic properties of most materials.) Different energy characterisations are derived for the heat exchanger with and without faults.

1.3.3 Graph matching approach

There are various graph matching techniques that can be applied. Attributed graph matching is chosen as the most suitable. The appropriate size for the attributed linear graph is identified and then populated with the energy information obtained in the previous step. This is done for the heat exchanger with and without a fault. Then, graph matching is applied to the different linear graphs, where each graph containing fault information is compared to the graph without fault information. The graph matching technique is applied by making use of MATLAB®.

1.3.4 Energy visualization

By making use of the data obtained by applying the graph matching technique, an energy signature of the heat exchanger without a fault can be obtained. The same procedure is then followed to obtain fault visualisations. The reference signature and fault energy visualisation will be compared and a procedure developed that will be able to distinguish between the different faults. The signatures will be created by making use of eigenvalue theory and will be implemented in MATLAB®.

1.3.5 Verification

The verification process will be spread out through the dissertation. Each consecutive outcome will be verified straight away to determine if the data or the information attained is sensible and meaningful.

1.4 Overview of dissertation

In chapter 2 an overview of heat exchanger types and faults are discussed. Some fault diagnosis schemes are examined. Then, energy concepts such as exergy, energy flow and heat transfer are described. An overview of different graph matching techniques is presented. Lastly, the basic mathematical equations of graph matching are explained.

The heat exchangers models that will be used are discussed in chapter 3. The staggered grid approach and the software package Flownex® are introduced. Attention will be given to how the fault models are constructed as well as the identification of the parameters that are available to be used.

Chapter 4 describes how the Flownex® model and its parameters will be translated into representing the energy in the heat exchanger. Energy characterisation will be calculated for the heat exchanger without a fault as well as each of the three faults.

In chapter 5 the energy characterisations of the previous chapter will be linked to linear graphs and a graph matching technique that makes use of local descriptions will be applied to the graphs. The technique compares two graphs by making use of node signature extraction. A cost matrix and distance parameter is defined for each set of graphs.

In chapter 6 the energy signatures and energy visualisations are calculated and displayed. The procedure to identify the different faults is described. The procedure is verified by using different boundary conditions and degrees of faults.

Finally, chapter 7 contains a discussion of the usefulness of using graph matching as a means to energy visualisation. Some concluding remarks and future work concerning this study is discussed.

Chapter 2

Literature overview

This chapter is concerned with the relevant literature associated with a graph theoretic approach towards energy visualisation of heat exchangers. The first part includes a literature survey regarding energy-based modelling and graph-theoretic system approaches. The chapter continues with some theory of heat exchangers and faults that occur on heat exchangers. Fault diagnosis is discussed briefly before continuing with energy concepts. Graph matching is considered next. The chapter concludes with a critical overview of the associated literature.

2.1 Literature Overview

Most large scale industrial processes take place in different physical domains. The challenge is to represent models of these systems in a standardised way representative of all relevant physical domains. Recent work that was done by Van Schoor et al in [9] suggests that energy is a sufficient tool to characterise and model large-scale industrial processes. Energy is described as a unifying concept that can be used across domains.

In 2011, Haddad and Nersesov [10] proposed a dynamical system model that is based on an energy perspective. Such a model is achieved by ensuring the model satisfies energy conservation laws. They then continue with this model and use an energy perspective to optimise a

large complex system whilst keeping in mind the stability and control of the system.

The problem of modelling a large system in multiple domains was already identified in 1984 by Chinneck and Chandrashekar [11]. They argue that a plant-level model is necessary in order to optimise a system. The plant-level models they developed relied strongly on the second law of thermodynamics - specifically in its exergy form. A set of variables that can sufficiently describe all energy flow in sub-systems was suggested by making use of exergy principles.

Concerning the use of energy for fault diagnosis, recent work by Marais et al [12] proposed an energy parameter to perform condition monitoring on a chemical reactor. The paper confirmed that the use of such an energy parameter has promise and that the parameter is sensitive to time domain variations. An important outcome was noted; the use of an energy parameter reduces the input space dimension.

Persin and Torvornik [13] focused on the detection of faults in a heat exchanger by making use of an analytical model. They made use of a velocity-based linearisation to take into account the non-linearity of the heat exchanger. In their study they based the linear observer on energy balance equations. The fault diagnosis of the heat exchanger was achieved in real-time.

The work of Uren and van Schoor [14] gives an example of fault detection on a heat exchanger by making use of energy-based visualisation. A state space model for a heat exchanger is derived along with state space models that include a fault. They then introduce an energy-based residual for both the steady state and transient response of the heat exchanger. Making use of an energy-based visualisation, they found that they could uniquely identify faults for the heat exchanger in steady state.

Concerning the use of a graph-theoretic approach, Reinschke argued that the modelling of a control system by making use of a graph overcomes the drawbacks of the state space approach [15]. In using a graph, system properties are assigned as the attributes. He argues that the graph-theoretic approach is especially suited to sparse large scale systems. He specifically uses directed linear graphs and inspects how linear graphs compare to state space models and other matrix structures.

Schmitke and McPhee proposed the use of a graph theory formulation to model a multi body,

multi-domain system in order to obtain the dynamics of the system [16]. They found that using a graph approach for this application led to reduction in model order. This enables the use of more complex systems as the equations that must be solved are reduced in order and are easier to handle by a computer.

Varga et al makes use of directed graphs to represent a network of heat exchangers [17]. The directed graphs are used to study the dynamics of the system and deliver a verdict on structure control properties such as controllability, observability and stability.

Leitold et al take it a step further and uses variable structured graphs to simplify dynamic process models [18]. The structured graphs are attributed direction graphs. They prove that they can simplify a process (with the use of graphs) whilst structural controllability and observability remain intact.

Concerning the use of graph theory and fault diagnosis: Tu et al make use of graphs to diagnose faults in large systems [19] and Chessa and Santi use graphs for the fault diagnosis of faulty mobiles in ad-hoc networks [20].

2.2 Heat exchangers

Heat exchangers are used in various energy conversion and utilization applications including household, commercial and industrial processes [21]. A heat exchanger is a device that enables the transfer of heat from one fluid to another. The fluids involved are prevented from mixing with each other and are at different temperatures. Depending on the application, various heat exchanger designs exist. Heat exchangers are typically classified according to flow arrangement and configuration [3]. In this section, an overview of the most popular classifications of heat exchangers will be provided along with some heat transfer concepts. Some faults that can occur on a heat exchanger will be considered.

2.2.1 Classification of heat exchangers

Flow arrangements

Three types of flow arrangements are present in heat exchangers [22]. In a parallel flow arrangement, the hot and cold fluids flow in the same direction - both enter at the same terminal and exit at the same terminal. In a counter-flow arrangement, the hot and cold fluids flow in opposite directions. The cold fluid enters at the terminal where the hot fluid exists and vice versa. In a cross-flow arrangement, the hot fluid flows perpendicular to the cold fluid flow.

Popular configurations of heat exchangers

The most popular configurations include shell-and-tube, plate and double-pipe heat exchangers. Shell and tube heat exchangers constitute a large shell which houses a large number of tubes. The flow in the tubes, containing the hot fluid, are parallel to that of the shell, containing the cold fluid [3]. Baffles are placed in the shell to support the tubes and to ensure that the cold fluid flows across the shell, enabling augmented heat transfer [23].

Plate heat exchangers constitute series of corrugated plates on a frame. Gaskets are used to ensure that the cold and hot fluids flow in different plates so that mixing does not occur [3]. The design of a plate heat exchanger enables a more compact design, achieved with a large surface area in a small volume [24]. Each cold fluid plate is adjacent to two hot fluid plates which increases heat transfer efficiency. The number of plates can be adjusted to suit the requirements needed for the specific application.

Double-pipe heat exchangers are considered the simplest type of heat exchanger and constitutes two concentric pipes. The hot fluid is found in the inner pipe and the could fluid in the outer pipe. This configuration is suitable for applications where one or both fluids are kept at high pressures. Counter-flow is customary in double-pipe heat exchangers, with the exception that parallel flow is established when a constant wall temperature is required [25].

2.2.2 Heat transfer concepts

Heat transfer is the hallmark of heat exchangers. However, heat transfer occurs in different modes. The three basic heat transfer mechanisms are conduction, convection and radiation. Conduction is the transfer of heat within a substance. Convection is the transfer of heat between a solid substance and an adjacent moving liquid or gas. Heat transfer in the form of electromagnetic waves is known as radiation. A short discussion of each mechanism follows.

Conduction

Conduction heat transfer occurs at atomic and molecular levels. In a substance, when the particles interact, energy is transferred from the particles with higher temperatures to the particles with lower temperatures. This transfer of energy is known as conduction [22]. Fourier's law is the rate equation for heat conduction and given by

$$\dot{Q}'' = -k\frac{dT}{dx}, \tag{2.1}$$

where $\dot{Q}''$ is the heat flux and is the heat transfer rate per unit area specifically in the x-direction in W/m^2, k is the thermal conductivity of the substance in question in W/m·K and dT/dx is the temperature gradient in the x-direction in K/m [22]. If the temperature distribution is linear and an area is considered, Fourier's law can be rewritten as

$$\dot{Q} = kA\frac{\Delta T}{L}, \tag{2.2}$$

where $\dot{Q}$ is the heat rate in W, A is the area in m^2 and $\Delta T/L$ is the linear temperature gradient in K/m.

Convection

Convection describes the heat transfer between a solid and a moving liquid (or gas) and consists of conduction and fluid motion. If fluid movement is absent, the heat transfer between the two substances is pure conduction. Concerning the fluid motion, the convection heat transfer is greater at higher rates of fluid movement. Natural convection occurs when fluid movement can be ascribed to density differences, whilst forced convection occurs when fluid movement

can be ascribed to external means [3]. Newton's law of cooling is used for convection and is given by

$$\dot{Q} = hA_s(T_s - T_{surr}), \tag{2.3}$$

where $\dot{Q}$ is the convection heat transfer rate in W, h is the convection heat transfer coefficient in $W/m^2 \cdot K$, A_s is the surface area in m^2, T_s and T_{surr} are the temperatures in Kelvin of the surface and of the fluid sufficiently far from the surface respectively [3].

Radiation

Substances that are at a nonzero temperature emit heat energy. This is known as thermal radiation and the energy is in the form of electromagnetic waves. In a vacuum thermal radiation is most efficient. Unlike convection or conduction heat transfer, an intervening substance is not required for radiation [22]. The maximum rate of radiation of an ideal substance is given by the Stefan-Boltzmann law as

$$\dot{Q} = \sigma A_s T_s^4, \tag{2.4}$$

where $\dot{Q}$ is the radiation in W, σ is the Stefan-Boltzmann constant in $W/m^2 \cdot K^4$ and T_s is the absolute temperature of the substance surface [3]. The radiation of a substance that is not ideal is given by

$$\dot{Q} = \varepsilon \sigma A_s T_s^4, \tag{2.5}$$

where ε is the emissivity of the substance with values that range between 0 and 1 [3]. Thermal radiation can be emitted and absorbed. When the temperature of the surroundings, T_{sur} is taken into account, the net rate of heat transfer in Watt is given by

$$\dot{Q} = \varepsilon \sigma A_s (T_s^4 - T_{surr}^4). \tag{2.6}$$

2.2.3 Heat exchanger faults

Heat exchangers are very commonly used in practise and offer significant challenges for engineers. The first challenge is to select the configuration of heat exchanger to achieve a certain temperature [26]. For the second challenge, the configuration of the heat exchanger is known, but an analysis is needed to determine operational parameters. There are two main analysis methods that can be used to solve the aforementioned problems [26]. The first is the log

mean temperature difference (LMTD) method and the second is the effectiveness-NTU method [3]. However, both methods assume certain perfect conditions which are not practical in real systems. The absence of these perfect conditions can be described as faults. Three typical faults in heat exchangers are discussed next.

Fouling

Fouling is the accumulation of deposits on heat transfer surfaces. Deposits can be in the form of biological growth, corrosion products and sediments [25]. Fouling can be modelled as additional resistance. Fouling creates a pressure drop and increases the thermal resistance of a heat exchanger [26]. Impurities in the fluids are the most common reason for fouling. A fouling factor R_f is a measure of the thermal resistance introduced by fouling.

Fluid leak

A fluid leak is a weakness on a heat exchanger component, normally a pipe, plate or shell, that allows fluid to escape. Physically it manifests as a crack, hole, fissure or passage on the component. The efficiency of a heat exchanger can be greatly reduced if a sufficiently large leak is present, especially in systems where the fluids are under high pressure [27]. A leak in a system can also lead to environmental contamination or hazards, depending on the fluids used in the heat exchanger. Leaks are mostly caused by corrosion.

Heat leakage

A heat leakage is found when the outer surface of the heat exchanger is not perfectly insulated. In a double pipe heat exchanger, this normally occurs on the cold fluid side and allows conduction to take place between the cold fluid and the surrounding environment [28]. If a heat leakage is present on a heat exchanger, the actual performance could be quite different than the predictions. Additionally, a heat leakage degrades the heat exchanger efficiency [29].

2.3 Fault diagnosis

Fault diagnosis consists of three different steps. Noticing the occurrence of a fault in the system is the first step, called fault detection. The second step is fault isolation. In this step the fault location is determined. In the last step, fault analysis, the type of the fault is determined along with the cause of the fault and the magnitude [30]. There are four basic techniques in fault diagnosis which are described in the following sections [31].

Hardware redundancy based fault diagnosis

This technique makes use of redundant hardware to reconstruct the process in question. The outputs of the reconstructed process components are compared to the original component outputs. If there is a fault on a component, the outputs will differ, indicating a fault. The advantage of this technique is that it is very reliant and fault isolation is straightforward. The disadvantage is that the use of redundant components result in a very high cost [31].

Signal processing based fault diagnosis

The idea of signal processing based fault diagnosis is captured in the name. Signals of the system are processed in order to achieve fault diagnosis. This technique relies on the fact that process signals carry information pertaining to the character of the system. After processing the signals, fault information is extracted as symptoms. Typical symptoms include time domain functions and frequency domain functions. The efficiency of this technique is limited. This technique can only be applied to steady-state systems [30].

Plausibility test

The plausibility test uses the input and output of a certain subsystem or component. A simple physical law that describes the dynamics of the component or subsystem is considered. If the output corresponding to the input does not make sense in terms of the physical law, plausibility is lost. Loss of plausibility indicates a fault. This technique is limited to fault isolation and complex processes [30].

Model-based fault diagnosis

Model-based fault diagnosis makes use of the same principle as hardware redundancy based fault diagnosis except the hardware is replaced by a software model. The software is in the form of a model. The model can be analytical or knowledge-based. The output of the software modelled components can then be compared to the components of the physical system and a difference would indicate a fault. The model and the physical system run in parallel and the variance in the outputs are called residuals [31].

2.4 Energy and some thermodynamic concepts

The concept of energy was introduced by Newton when he worked on kinetic and potential energy [32]. Energy is a scalar quantity. Although energy is such a popular concept, one cannot observe energy. Rather, energy can be recorded and evaluated. The energy of a system also describes the internal energy of the system. This makes it difficult to measure the absolute energy of the system or calculate the potential of the system [32]. For this reason concepts, such as exergy and entropy have been introduced. In the following sections, energy is examined in more detail along with a discussion of some thermodynamic concepts.

2.4.1 Energy

As already stated, energy is a unifying concept and is representative of all domains. Signal analogies can be adopted and all the various signals of the different domains reduced to four basic variables [2]. The four variables are: effort e, flows f, generalised momenta p and generalised displacement q. Table 2.1 gives the four variables for the physical domains. The relationships between the four variables are given as

$$p(t) = p(t_0) + \int_{t_0}^{t} e(\tau)d\tau \quad \text{and} \tag{2.7}$$

$$q(t) = q(t_0) + \int_{t_0}^{t} f(\tau)d\tau, \tag{2.8}$$

where t_0 is the intial time. Each domain has two power variables, with the power given as

$$P(t) = f(t)e(t), \tag{2.9}$$

where $P(t)$ is the power, $e(t)$ is the effort variable and $f(t)$ is the flow variable. Energy is calculated from the integral if the power:

$$E(t) = E(t_0) + \int_{t_0}^{t} f(\tau)e(\tau)d\tau, \tag{2.10}$$

where $E(t)$ is the energy at time t and $E(t_0)$ is the initial energy.

Table 2.1: Domains and variables

Domain	**Effort** e	**Flow** f	**Generalised Displacement** q	**Generalised Momentum** p
Electric	Voltage	Current	Charge	Flux linkage
Translation	Force	Velocity	Displacement	Momentum
Rotation	Torque	Angular velocity	Angular displacement	Angular momentum
Fluid	Pressure	Volume flow	Volume	Pressure momentum
Thermodynamic	Temperature	Entropy flow	Entropy	NA

The first law of thermodynamics states that energy cannot be destroyed, it can only be transferred between forms. Equivalently stated, the change of energy in a system is the difference of the energy entering the system and the energy leaving the system [33]. In equation form:

$$\Delta E_{system} = E_{in} - E_{out}. \tag{2.11}$$

The above equation can be rewritten as

$$\Delta E_{system} = \Delta U + \Delta KE + \Delta PE, \tag{2.12}$$

where ΔU is the change in internal energy, ΔKE is the change is kinetic energy and ΔPE is the change in potential energy [33].

2.4.2 Exergy

The amount of possible work that one can extract from a system when it interacts with the surrounding environment is known as the exergy of the system [34]. The pressure and temperature from the surrounding environment is used as a reference and is denoted as P_0 and T_0.

Exergy is closely related to reversible work. Unlike energy, exergy can be destroyed. However, when all the processes in a system are reversible, exergy is conserved [32].

Exergy only exists when the system is not in equilibrium with the surroundings. Equilibrium indicates that the system and the environment are at the same temperature, pressure, concentration [32]. Exergy is also known as available energy, and for every form of energy transfer that exists, there is an equivalent form of exergy transfer. The problem with exergy is that it depends on the surroundings. Thus, care should be taken in defining the reference temperature and pressure accurately.

2.4.3 Entropy

The amount of molecular disorder in system is known as the entropy of the system [34]. Specific entropy is a thermodynamic property of a system and normally noted on tables along with specific volume, specific internal energy and specific enthalpy. Entropy is a fundamental concept in the second law of thermodynamics. The unit of specific entropy is kJ/kg·K and is denoted by s [33]. The entropy change between two states are always the same, independent of the path taken.

The second law of thermodynamics describes the quality of energy in a system and discloses that not all energy in a system can be used or transferred [32]. The Clausius inequality describes the second law mathematically by

$$\oint \frac{\delta Q}{dT} \leq 0, \tag{2.13}$$

where the cyclic integral is used to infer that integration should be done over the entire cycle [32]. Using entropy (2.13) can be rewritten as

$$S_{gen} = -\oint \frac{\delta Q}{dT}, \tag{2.14}$$

with S_{gen} is the entropy generation for the entire cycle. For a reversible process, (2.15) gives the entropy generation and (2.16) gives the entropy for a irreversible process:

$$S_{gen} = \Delta S_{total} = \Delta S_{sys} + \Delta S_{surr} = 0, \tag{2.15}$$

$$S_{gen} = \Delta S_{total} = \Delta S_{sys} + \Delta S_{surr} > 0, \tag{2.16}$$

with ΔS_{sys} the change in entropy of the system and ΔS_{surr} the change of entropy in the surroundings.

2.4.4 Enthalpy

Enthalpy is a thermodynamic property defined by

$$h = u + Pv, \tag{2.17}$$

where h is the specific enthalpy in J/kg, u is the specific internal energy in J/kg, P is the pressure in Pa and v is the specific volume in m^2 [34]. In the case of an ideal gas enthalpy is given by

$$h = u + RT, \tag{2.18}$$

where T is temperature in K and R are constants [34]. From (2.18) it is clear that the enthalpy of an ideal gas is only dependent on the temperature of that ideal gas.

2.5 Graph Matching

Graph matching was developed to find how similar structural descriptions of objects are [35]. Structural descriptions refer to a description of an object in terms of the different sections of the object, the properties of the different sections and how the sections pertain to each other. The most natural form of such a structural description is an attributed linear graph [36]. A linear graph constitutes of nodes and edges (that connects the nodes). In an attributed linear graph, the properties of the sections are placed as attributes of the nodes and the attributes of the edges describe how the sections relate to another. A weighted graph has only edge attributes. In a directed graph, the edges have a specifc direction. Graph matching is a technique that can be used to determine graph similarity. The idea is to find a similarity between graphs in such a way that the process that finds correlations between the different attributes and nodes does it as consistently as possible [35].

The following sections will provide some background on graph matching and the basic mathematical equations used in graph matching for pattern recognition will then be included.

2.5.1 Graph matching background

Various approaches have been used to derive the similarities between two graphs. In 1979, Tsai and Fu presented an approach for finding isomorphisms between graphs that included both numeric and symbolic attributes [37]. They made use of the tree search techniques as did [38]. Both these techniques gave optimum matchings, but large graphs would present a problem due to the combinatorial nature of the techniques.

In 1988, Umeyama presented an analytic technique that depends on the eigen-decomposition of the adjacency matrix [39]. His technique could handle larger graphs but is restricted to numerical weighted graphs (node attributes are not handled). The technique is limited in that graphs cannot differ significantly close. Umeyama's technique falls under the category of non-linear optimisation methods.

Non-linear optimisation methods that make use of relaxation labelling include [40], [41] and [42]. Other non-linear optimisation are polynomial transforms [6], graduated assignment [43] and neural networks [44–46].

2.5.2 Graph matching in pattern recognition

Graph matching is widely used in the application of pattern recognition. According to [35] the most popular and comparable techniques that use full graph matching (number of nodes are alike) and where the graphs have multiple attributes include:

- Graduated assignment graph matching [43].
- Eigen-decomposition graph matching [39].
- Linear programming graph matching [47].
- Polynomial transform graph matching [6].
- Least squares graph matching [48].
- RKHS interpolator graph matching [49].
- Spherical approximation graph matching [50].

- Faugeras-price relaxation labelling [51].
- Interpolater-based Kronecker product graph matching [35].

2.5.3 Basic mathematics

The basic equations and principles for attributed graph matching as used in pattern recognition will be discussed in this section and is based on the work of [52].

Let G' be a reference graph and G be a duplicate graph each with n nodes, represented by

$$G' = (V', E', \{\mathbf{A}'_i\}_{i=1}^{r}, \{\mathbf{B}'_j\}_{j=1}^{s}), \tag{2.19}$$

$$G = (V, E, \{\mathbf{A}_i\}_{i=1}^{r}, \{\mathbf{B}_j\}_{j=1}^{s}), \tag{2.20}$$

where V is the set of vertices of the graph, E the set of edges of the graph, $A_i \epsilon R^{n\times n}$ is the edge attribute adjacency matrix associated with the ith edge and $B_j \, \epsilon \, R^{n\times 1}$ the vertex attribute vector associated with the jth matrix. Equivalently for G'. r is the number of attributes per edge and s is the number of attributes per node.

In the case of attributed graph matching where G and G' have the same number of nodes, G is matched to G' by finding a permutation matrix $\mathbf{P}$ such that

$$\mathbf{A}_i = \mathbf{P}\mathbf{A}'_i\mathbf{P}^T \tag{2.21}$$

for i = 1,...,r and

$$\mathbf{B}_j = \mathbf{P}\mathbf{B}'_j \tag{2.22}$$

for j = 1,...,s. (2.21) and (2.22) are however not very realistic, so noise matrices $\mathbf{N}_i$ and $\mathbf{M}_j$ are added:

$$\mathbf{A}_i = \mathbf{P}\mathbf{A}'_i\mathbf{P}^T + \epsilon\mathbf{N}_i \tag{2.23}$$

for i = 1,...,r and

$$\mathbf{B}_j = \mathbf{P}\mathbf{B}'_j + \epsilon\mathbf{M}_j \tag{2.24}$$

for j = 1,...,s. ϵ is related to noise power and is assumed to be independent of i and j. The general attributed graph matching problem can now be formulated. The idea is to find a permutation

matrix $\mathbf{P}$ for some norm $||\cdot||$ that satisfies:

$$min(\sum_{i=1}^{r} W_i||\mathbf{A}_i - \mathbf{P}\mathbf{A}'_i\mathbf{P}^T||^q + \sum_{j=1}^{s} W_j||\mathbf{B}_j - \mathbf{P}\mathbf{B}'_j||^q), \tag{2.25}$$

where $\{W_i\}_{i=1}^{r+s}$ is a set of non-negative weights such that

$$\sum_{i=1}^{r+s} W_i = 1. \tag{2.26}$$

2.6 Critical overview and conclusion

The focus of this research study is on heat exchangers, fault diagnosis, energy concepts and graph matching. A broad overview of these aspects was introduced and discussed in this chapter.

The classifications, heat transfer concepts and faults of heat exchangers were examined. The double pipe heat exchanger was highlighted as one of the simplest heat exchangers. Attention was given to three common faults that occur in heat exchangers: a fluid leak, heat leakage and fouling. These faults will be focussed on during fault diagnosis. Next, four basic techniques of fault diagnosis were discussed. It can be noted that the signal based and model based techniques are the most suited for the purposes of this study.

Energy as a multi-domain parameter was discussed. Some other concepts such as exergy, entropy and enthalpy were also considered. It was revealed that using the principle of energy in modelling would be a beneficial attempt. A key aspect of using energy is that it leads to data reduction, which is of great significance in the field of fault diagnosis. Although, energy has certain shortcomings; utilising the concept of exergy could disclose more characteristics of a system.

Various graph matching techniques were considered. It is noted that the use of graph matching techniques as applicable to pattern recognition would be of most value in this study. The basic idea of attributed graph matching for pattern recognition was explained in terms of mathematical equations.

Some literature regarding this study was not considered in this chapter. The following chapters will discuss important concepts and background as necessary.

Chapter 3

System Model

This chapter is concerned with the heat exchanger model that will be used. The staggered grid approach that is applied to obtain the model in Flownex® is discussed along with components that are used to realise the system and the properties of these components. Then, the faults that will be induced on the heat exchanger and the components that are needed to realise these faults are discussed. The chapter concludes with the properties of the model that are available to be used for the rest of the study.

3.1 Physical system description

The model is based on a CO_2 heat pump test bench at the North-West University's school of Mechanical Engineering. Figure 3.1 depicts the system. The numbers from 1-5 are used to depict the different components. The system constitutes a gas cooler (1), a compressor (2), an expansion valve (3) and an evaporator (5). The gas cooler is a counter-flow double pipe heat exchanger and the focus of this study. The schematic diagram of the heat exchanger is shown in Figure 3.2.

Flownex® is the software package that will be used to model the heat exchanger. The simulation environment of Flownex® is suited to simulate flow and heat transfer systems [53]. A Flownex® model for this specific gas cooler has already been done by Smuts in [54]. The model

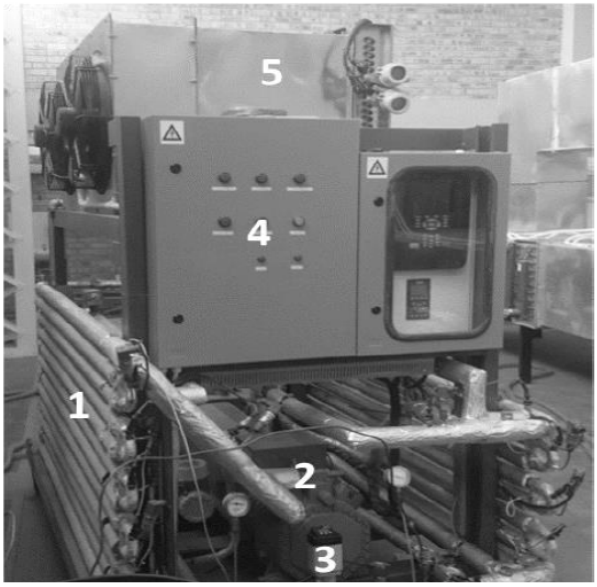

Figure 3.1: CO_2 heat pump test bench

used in this study as well as the assumptions are based entirely on the work done by Smuts.

3.2 Modelling approach

3.2.1 Requirements of the model

A model is required in order to obtain a visualisation of energy in the heat exchanger. This is done for the purpose of fault detection. Since the idea is to do this for a physical system, all parameters needed must be based on sensor data and geometric properties that can be obtained from the physical system. The available sensor data include temperatures, pressures and mass flow at certain points in the system. For this reason, the model must be relatively simple. Another requirement of the model is that it must be easily realisable in Flownex® by the components that are available.

3.2.2 Methodology

In order to satisfy the above requirements and as sensor data is available only for certain points; for the sake of simplicity, a two-dimensional approach to model the heat exchanger is used.

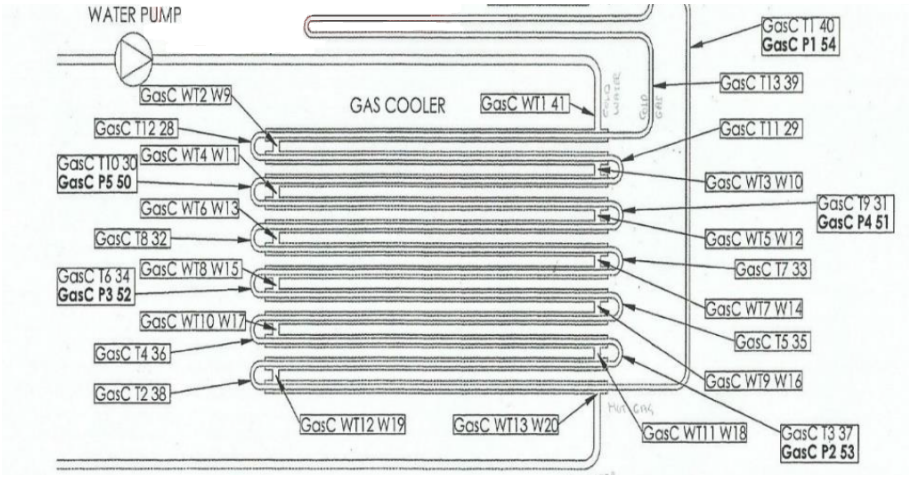

Figure 3.2: Schematic of test bench gas cooler [54]

The verification and validation that was done on the model by Smuts [54] has shown that a two-dimensional approach is a realistic representation of the real system for the purposes of this study. From the schematic (Figure 3.2) it is clear that the gas cooler is a double pipe heat exchanger with two concentric pipes. For modelling purposes, this configuration can be adapted to a side-by-side pipe configuration as depicted in Figure 3.3.

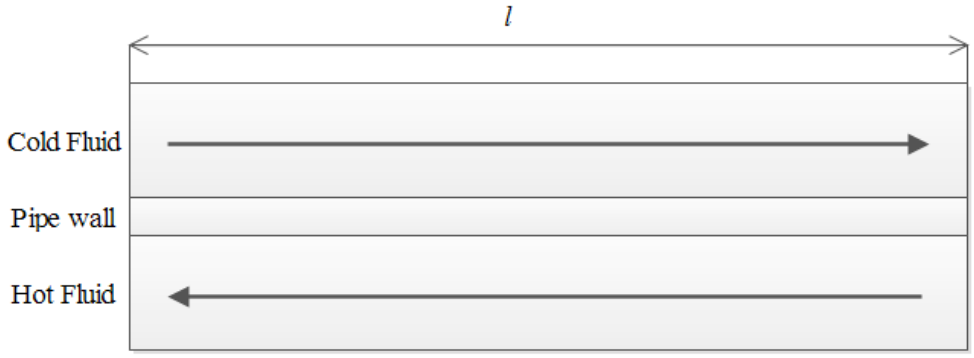

Figure 3.3: Two-dimensional layout of the heat exchanger for modelling purposes

The total length of the heat exchanger pipes is denoted in meter by l. In order to link this model to a system that is realisable in Flownex®, the staggered grid approach of Patankar [55] is applied to Figure 3.3 resulting in the representation depicted in Figure 3.4. As the figure shows, the pipe is divided into two main grid points for each of the cold fluid, hot fluid and separation wall. The assumption is made that heat transfer between the hot and cold fluid only takes place at these main grid points. Following this approach, a control volume is defined around main grid points and secondary grid points are inserted between main grid points. As

depicted in Figure 3.4 the rectangles denote the main grid points and the parameters that are known in these points are temperature and pressure. The circles denote the secondary grid points and the mass flow rate is known at each of these points. Main grid points are denoted by M and secondary grid points by S.

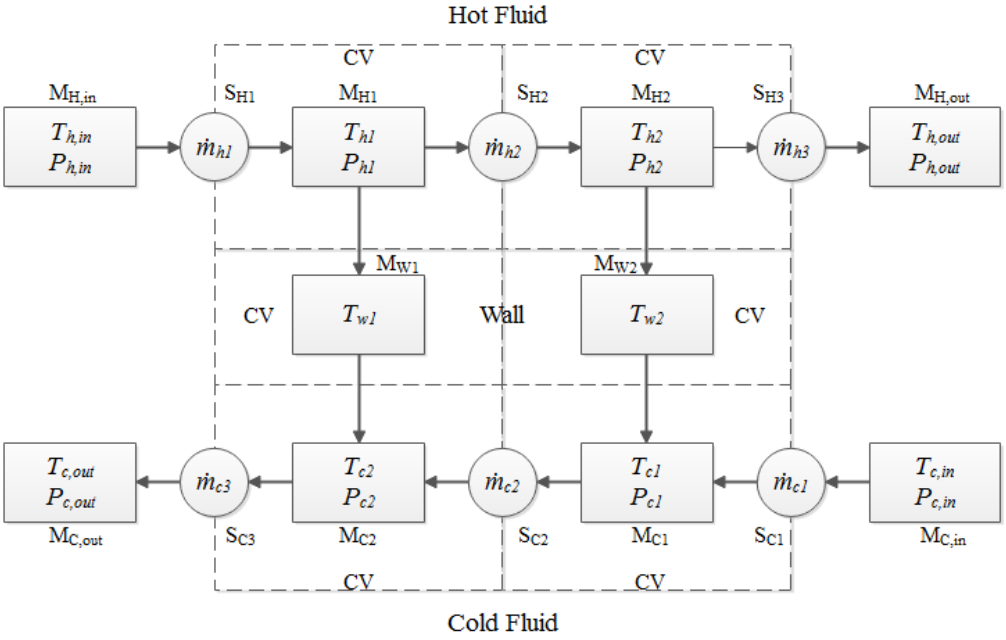

Figure 3.4: Representation of the staggered grid modelling approach applied to the heat exchanger

The next step is to realise the above approach in Flownex® as explained in more detail in the next section along with the model parameters required to set up the model and some assumptions that were made.

3.3 Model components, parameters and assumptions

The Flownex® model of the heat exchanger is depicted in Figure 3.5. In the model, pipes are used to represent secondary grid points of the staggered grid approach and nodes are used to represent main grid points. In the pipes, mass flow will be calculated and on the nodes, temperatures and pressures will be calculated.

In order to model the separation wall, conduction nodes are used to mimic the conduction

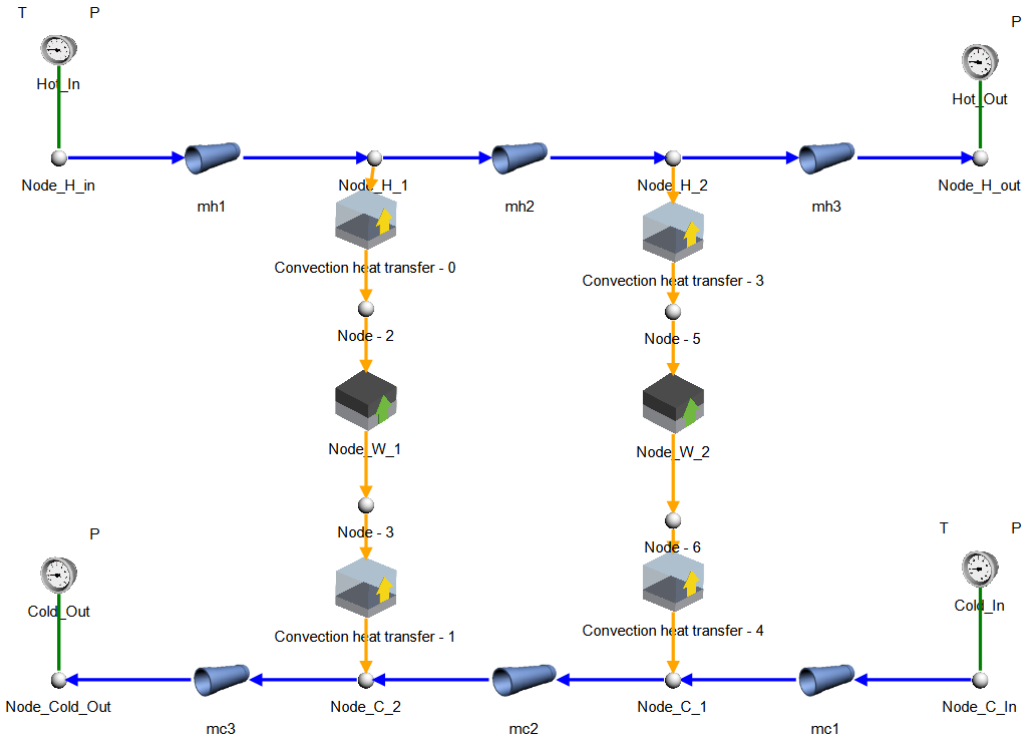

Figure 3.5: Flownex® model of heat exchanger

through the wall, and to model the heat transfer between the fluids and the wall, convection heat transfer components are used. Boundary condition components are used to specify the inlet temperatures and pressures for the hot and cold fluids and the outlet pressures for the hot and cold fluids. The rest of the parameters and assumptions needed are discussed in the sections that follow.

3.3.1 Boundary conditions

The nature of the physical system is such that the parameters that can be specified for the hot fluid pipe include the inlet temperature, the inlet pressure and the outlet pressure. For the cold side, the inlet temperature, inlet pressure and outlet pressure can be specified. This model is based on a single phase heat exchanger, thus it is important to note that the boundary conditions must be specified in such a way that the hot fluid, which is CO_2, remains in the gas phase and the cold fluid, which is water, remains in the liquid phase. In this study the boundary conditions are adjusted to generate data for different cases. The boundary conditions used for validation of the model are discussed in section 3.4.

3.3.2 Pipe parameters

The length of the physical system is 24 m. As the model constitutes three pipe sections, each will have a length of 8 m. Table 3.1 shows the pipe diameters as calculated for the side-by-side layout. These properties are based on the model by Smuts [54].

Table 3.1: Geometry of the pipes

Parameter	**Value**	**Unit**
Hot pipe inner diameter	15.8	mm
Hot pipe wall thickness	2.75	mm
Cold pipe inner diameter	15.933	mm
Cold pipe wall thickness	3.4	mm

Assumptions that were made for the pipe components include:

- Young's modulus is taken as zero.
- The Darcy-Weisbach friction factor of the pipes are constant with a value of 0.026.
- The cold fluid pipe is perfectly insulated against the environment.

3.3.3 Heat transfer parameters

The separation wall for the heat exchanger is AISI 304 stainless steel. It is assumed that the density and specific heat of all fluids are constant for this study. Furthermore, it is also assumed that the heat transfer is perfectly uniform and the heat transfer coefficients remain constant.

Table 3.2 shows the properties that are specified for the heat transfer components in Flownex®.

Table 3.2: Heat transfer properties

Property	Value	Unit
Convection coefficient M_{H1}	2871	$W/m^2.K$
Convection coefficient M_{H2}	4185	$W/m^2.K$
Convection coefficient M_{C1}	3510	$W/m^2.K$
Convection coefficient M_{C2}	4300	$W/m^2.K$
Heat transfer area M_{H1}	0.5956	m^2
Heat transfer area M_{H2}	0.5956	m^2
Heat transfer area M_{C1}	0.803	m^2
Heat transfer area M_{C2}	0.803	m^2

3.3.4 Fluids used

In Flownex® the hot fluid is chosen as ”CO2 - Carbon Dioxide” which is then specified as a pure compressible gas. It has a molar mass of 44.01 kg/mol and a critical pressure of 7377 kPa. The density, viscosity, enthalpy and entropy are all calculated by Flownex® by making use of predefined tables.

The cold fluid is chosen as ”H2O - Water” which is a two phase fluid and uses all the predefined properties of Flownex®.

3.4 Validation of the model

The model validation was done by Smuts in [54]. This was done by comparing the results from the Flownex® model to data obtained from experiments on the physical test bench at the North-West University which was described at the beginning of the chapter. The initial conditions that were used for validation are given in Table 3.3.

Table 3.3: Flownex® model validation initial conditions

Parameter	Value - Experiment 1	Value - Experiment 2	Unit
Hot side inlet pressure	6890	7190	kPa
Hot side outlet pressure	6510	6780	kPa
Cold side inlet pressure	286	286	kPa
Cold side outlet pressure	250.95	250.95	kPa
Hot side inlet temperature	330.25	334.85	K
Cold side inlet temperature	288.55	288.55	K
Hot side mass flow rate	0.169	0.187	kg/s
Cold side mass flow rate	0.267	0.267	kg/s

3.5 Fault models

In this section the faults of the heat exchanger will be discussed, this includes the parameters that are adjusted or components that are added in order to simulate a fault. The faults that are modelled include a model with a heat leakage, a model with a fluid leak and a model with fouling in the cold fluid pipe.

3.5.1 Model with fluid leak

In order to model a fluid leak; a small pipe is added to the cold fluid pipe. This pipe allows fluid to flow out of the heat exchanger. The Flownex® model for a leak is depicted in Figure 3.6, only the cold fluid side is shown.

Table 3.4 gives the geometry of the pipe used to model the leak. The boundary conditions that are used for the outlet side of the pipe is the ambient pressure and temperature taken as 100 kPa and 300 K respectively.

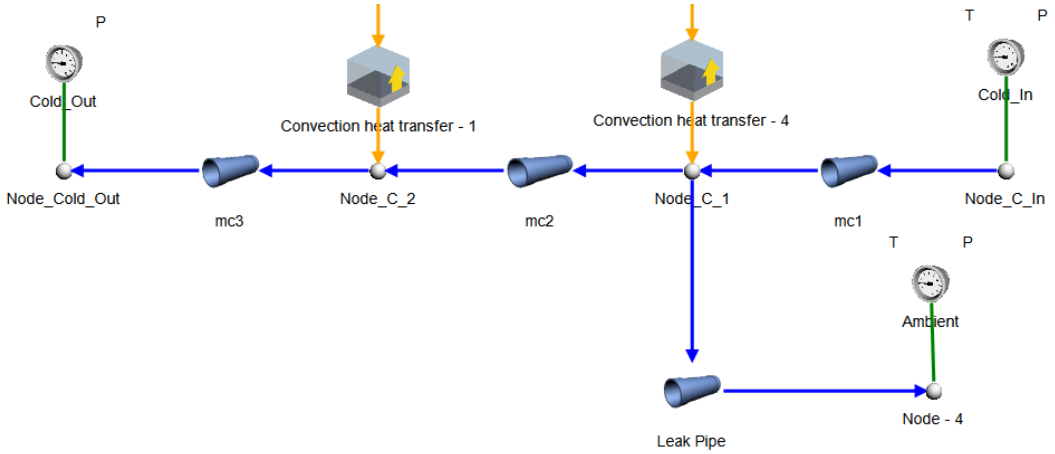

Figure 3.6: Flownex® model with fluid leak

Table 3.4: Geometry of the fluid leak pipe

Parameter	Value	Unit
Leak pipe diameter	1	mm
Leak pipe length	2.75	mm

3.5.2 Model with heat leakage

In order to model the heat exchanger with a heat leakage fault, a convection heat transfer component is added to the model. This component allows heat to be dissipated into the environment. The Flownex® model with heat leakage is depicted in Figure 3.7.

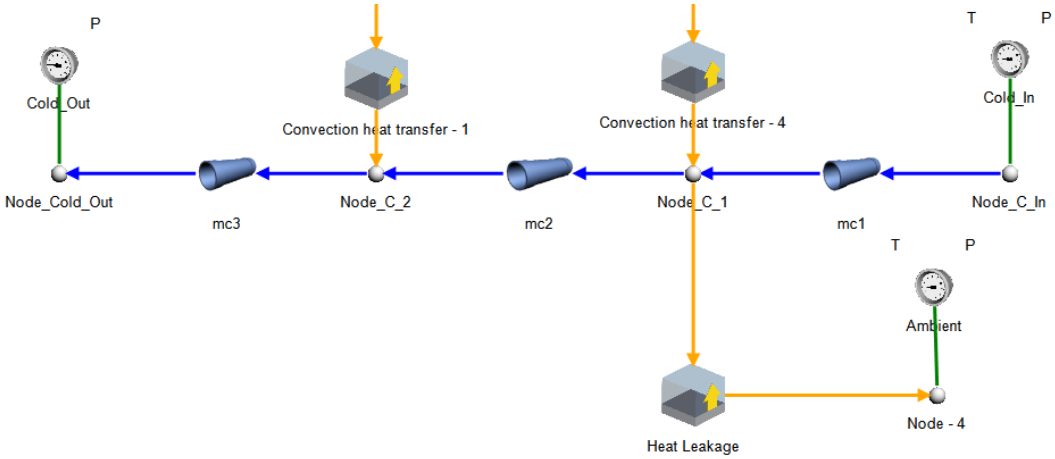

Figure 3.7: Flownex® model with heat leakage

Table 3.5 provides the properties used to model the heat leakage. The boundary conditions for the convection component is the ambient pressure and temperature taken as 100 kPa and 300 K respectively.

Table 3.5: Properties for heat leakage component

Parameter	Value	Unit
Wall 1 heat transfer coefficient	4300	$W/m^2.K$
Wall 2 heat transfer coefficient	3510	$W/m^2.K$
Wall 1 & 2 heat trasnfer area	0.803	m^2

3.5.3 Model with fouling

In order to model a heat exchanger where fouling is present in the cold fluid pipe, the model remains as described in section 3.3 accept that the K forward parameter of the pipe is adjusted from zero to a positive value. Fouling is generally modelled by making use of the K-forward factor and relates to an increase of flow resistance. In this specific case it is adjusted to 30. The value is adjusted for all three pipe components in the Flownex® model.

3.5.4 Comparison of different models

The different models as described are simulated with the same boundary conditions. Table 3.6 depicts the change in some of the key grid points. The values given are obtained from the model after steady state has been reached.

When a comparison is made between the normal model and the fault models, it is clear that there is a difference in parameters values. When the values of the different fault models are compared, it can be seen that parameters stay the same for some faults and for other parameters differences are noted.

Table 3.6 verifies that for different faults, the parameters change as expected at the relevant places. Additionally, the table confirms that some parameter values remain constant as predicted beforehand.

Table 3.6: Comparison of models

Parameter	Normal	Leak	Heat leak	Fouling	Unit
M_{H1} pressure	7916	7915.8	7907.4	7921.8	kPa
M_{H2} pressure	7849.2	7848.8	7837.6	7854	kPa
M_{C1} pressure	283.05	282.51	283.04	283.07	kPa
M_{C2} pressure	280.08	279.81	280.08	280.10	kPa
M_{H1} temperature	356.3	356.4	349.8	367.7	K
M_{H2} temperature	330.3	329.7	319.0	341.0	K
M_{C1} temperature	320.1	319.2	304.6	331.8	K
M_{C2} temperature	342.3	342.4	332.3	358.5	K
Hot side mass flow rate	0.251	0.251	0.263	0.242	kg/s
S_{C1} mass flow rate	0.134	0.146	0.134	0.0735	kg/s
S_{C2} mass flow rate	0.134	0.128	0.134	0.0735	kg/s
S_{C3} mass flow rate	0.134	0.128	0.134	0.0735	kg/s
Wall temperature 1	347.5	347.6	338.7	361.19	K
Wall temperature 2	325.0	324.2	311.5	336.2	K

Concerning the mass flow rate on the cold side, it is clear that there is a loss of mass flow between secondary grid points S_{C1} and S_{C2} for the fluid leak case. For all other cases, the mass flow rates are the same for all secondary grid points. The hot side mass flow rates are the same in all the secondary grid points of the hot side and thus only one reading is included in the table. For the case of fouling, the mass flow rate in the cold pipes are significantly smaller than for the other cases, this is due to fouling in the pipes which results in an increase in flow resistance.

Concerning the temperature of the main grid point of M_{C2}, in the case of a heat leakage, the temperature falls with 10 K when compared to the normal case. This is due to the heat that is transferred to the environment. In the case of fouling, the temperature is more by about 16 K (compared with normal case). This is ascribed to the diminished flow rate, which means less cold water is flowing though the pipes, resulting in less heat transfer.

3.6 Parameters needed for energy characterisation

A purpose of this study is to identify the faults that occur on a physical heat exchanger by making use of sensor data available. Even though multiple thermodynamic and fluid properties are available from the Flownex® models discussed in this chapter, only a certain number of parameters can be chosen to use in the energy characterisation discussed in the next chapter.

The parameters that are deemed crucial relating to energy characterisation include:

- The hot side inlet pressure.
- The hot side inlet temperature.
- The hot side outlet pressure.
- The cold side inlet pressure.
- The cold side inlet temperature.
- The cold side outlet pressure.
- The mass flow rates in all pipes.
- The temperatures and pressures of the control volumes M_{H1}, M_{H2}, M_{C1} and M_{C2}.
- Geometric properties.
- Heat transfer coefficients.

Most of the above parameters are measured by sensors. In the cases where sensor data are not available, the specifications and geometries of the heat exchanger can be used to calculate the values. For example, the heat transfer coefficients will not be measured by sensors, but are calculated beforehand and assumed as constant.

3.7 Conclusion

The development of a Flownex® model for a counter-flow heat exchanger was discussed in this chapter. In stead of making use of actual measured data, the validated model will be

used throughout the study. The use of a model enables the simulation of various boundary conditions and other cases that will be considered. Certain assumptions were made in order to simplify the model and must be kept in mind for the rest of the study. Although the two-dimensional approach is a substantial simplification, the model is deemed realistic for further work. Future work could include the use of a more complex model. Parameters that are available from sensor data or those that can be calculated, were identified. These parameters can be used for energy characterisation.

Chapter 4

Energy characterisation

This chapter is concerned with the energy characterisations of a heat exchanger. The energy characterisations are obtained by making use of the model developed in the previous chapter. The use of entropy, enthalpy, exergy and energy flow rate in energy equations are discussed. The chapter continues with a description of how software is utilised to obtain and calculate required values. Lastly the energy characterisations for the heat exchanger with and without faults are discussed for a specific set of boundary conditions.

4.1 Exergy and energy flow rate

In Chapter 2 it was determined that it is useful to examine the energy in a system for various reasons. Nevertheless, working with energy itself as a system property poses difficulties. In fact, energy cannot be used to represent a quantity that calculates the work potential of a specific component, system or material. Consequently, it would be desirable to work with a property that can determine the amount of useful work potential a system, component or material has. This property is called exergy and is the amount of energy that can be converted to work between two states.

Now, exergy can describe the available energy at a point in a system, but how the energy is

transferred between sub-systems or components is also of interest. Therefore, it is proposed that an energy flow rate is used along with exergy. Energy flow rates describe how energy is transferred between subsystems or components. According to [11], all forms of energy in a system can be conveyed by making use of exergy and energy flow rate. It is assumed that the kinetic and potential energy remain constant. The energy flow between two points in a thermo-hydraulic system is given by

$$\dot{q}_{12} = \dot{m}_{12}(h_1 - h_2), \tag{4.1}$$

where $\dot{q}_{12}$ is the energy flow (W), $\dot{m}_{12}$ is the mass flow rate (kg/s) and h_i is the specific enthalpy of point i in (J/kg) [11]. The specific exergy at a point in a thermo-hydraulic system is given by:

$$x = (h - h_0) - T_0(s - s_0), \tag{4.2}$$

where x is the specific exergy (J/kg), h the specific enthalpy (J/kg), h_0 the specific enthalpy of the reference state (J/kg), T_0 the temperature of the reference state (K), s the specific entropy (J/kg.K) and s_0 the specific entropy of the reference state in (J/kg.K) [56].

In this specific study, the heat transfer from the hot liquid to the cold liquid is also of importance and is given by

$$\dot{q} = UA(T_1 - T_2), \tag{4.3}$$

where $\dot{q}$ is the heat transfer rate (W), U the heat transfer coefficient (W/m^2.K), A the area (m^2) and T the temperature (K) [22].

Equations (4.1), (4.2) and (4.3) provide a procedure to represent the energy in a system by making use of enthalpy, entropy, temperature, mass flow rate and some geometric properties. As discussed in the previous chapter, only pressures, temperatures, mass flow rates and the geometric properties are known. As a result, a way must be found to obtain enthalpy and entropy values from the parameters that are available. This is discussed in the next section.

4.2 Entropy and enthalpy

Entropy and enthalpy are thermodynamic properties, as such there is a relationship between the pressure and temperature of a material and its enthalpy or entropy. A schematic for the T-s diagram (temperature - entropy) for water can be seen in Figure 4.1 which shows a relationship

between entropy, temperature and pressure or volume. The solid black line provides information of the phases of the substance. Inside the black dome, water and steam exist together, this is known as the liquid vapour region. Outside the dome and to the left of the critical point is the liquid region. Outside the dome and to the left of the critical point is the gas region. At the critical point, both liquid and gas have the same density. Lines of constant pressure are denoted with solid pink lines. Everywhere on these lines, the pressure remains the same, even though the entropy and temperature changes. Lines of constant density are denoted with dashed pink lines. Using T-s diagrams, one can find the entropy that belongs to a specific pressure and temperature.

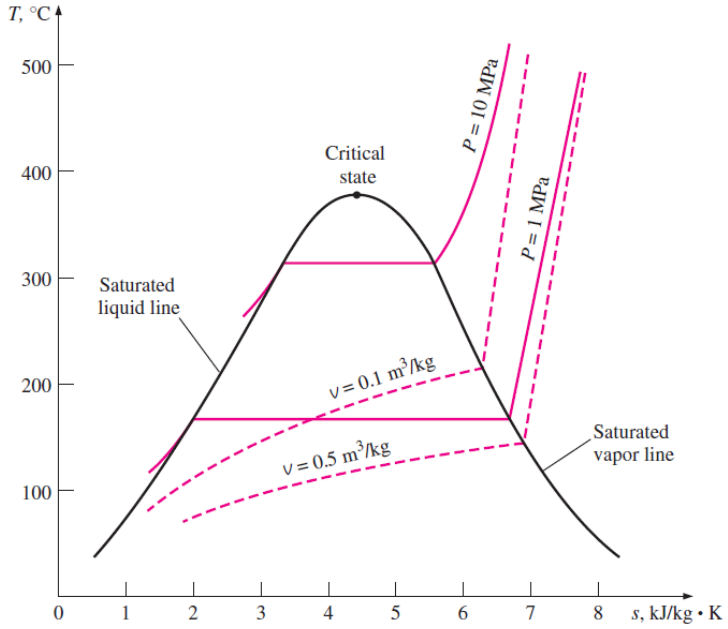

Figure 4.1: Schematic of the T-s diagram for water [56]

Diagrams that link temperature and pressure with enthalpy also exist. In addition, extensive tables exist that can be used to calculate the entropy and enthalpy of a substance at a specific temperature and pressure. Consequently, the relationships that exist between thermodynamic properties provide a way in which the heat exchanger properties and parameters available (from the Flownex® model) can be used to create an energy characterisation of the system in terms of exergy and energy flow rate. Table 4.1 shows the enthalpy and entropy values of CO_2 and H_2O for different temperature and pressure sets.

Table 4.1: Entropy and enthalpy for some points

Fluid type	**Pressure [Pa]**	**Temperature [K]**	**Enthalpy [J/kg]**	**Entropy [J/kg.K]**
CO_2	8913100	363.03	499470	1934
CO_2	8845900	330.85	444060	1752
H_2O	283060	316.11	180130	612
H_2O	280090	344.90	300610	976

4.3 Computational platforms

In order to obtain and compute the energy characterisation of the heat exchanger, computational platforms are used. EES (Engineering Equation Solver) is a software package that can be used to solve algebraic and differential equations. Among other things it can also be used to compute thermodynamic properties of materials by using a thermodynamic and transport property database. For this specific study, the functions *"enthalpy"* and *"entropy"* are used. The input parameters are the material name, the temperature and the pressure. The aforementioned inputs are obtained from the Flownex® model.

Furthermore, MATLAB® is used for all other computations. Moreover, MATLAB® provides the functionality to call the EES functions above by making use of EES Macro files. The Macro files are given in Appendix A. Furthermore a memory link can be created between Flownex® and MATLAB® and thus experimental data from the model can be stored in MATLAB® and accessed directly. Figure 4.2 depicts the interaction between the software platforms.

Step 1: Boundary conditions are set in Flownex®.

Step 2: By making use of the memory link, parameters such as temperatures, pressures, mass flow rates and heat transfer coefficients are imported into MATLAB® from Flownex®.

Step 3: MATLAB® saves and orders the parameters.

Step 4: Temperatures, pressures and the names of the materials are sent to EES.

Step 5: EES calculates the enthalpy and entropy values.

Step 6: Enthalpy and entropy values are imported in MATLAB®.

Step 7: Equations (4.1) - (4.3) are applied to the relevant parameters to obtain the exergy and energy flow at certain points in the system.

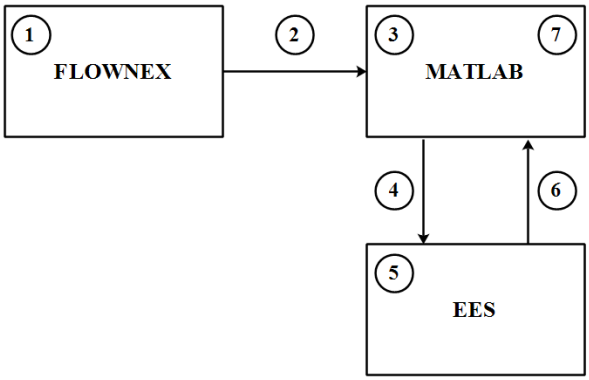

Figure 4.2: Software interaction of computational platforms

In (4.1) and (4.2), a reference state enthalpy and entropy are used. The reference state is chosen as 100 kPa and 300 K. Thus the reference state's enthalpy, h_0, and entropy, s_0, are calculated for the hot fluid, the cold fluid and the wall and are then used in the calculations to obtain the exergy at that specific point. The enthalpy and entropy of the reference state fro the different fluids and materials are given in Table 4.2.

Table 4.2: Entropy and enthalpy values for the reference state of 100 kPa and 300 K

Material	**Enthalpy [J/kg]**	**Entropy [J/kg.K]**
H_2O	112650	393
CO_2	507440	2745
Stainless Steel	88733	585

As a result of the reference state chosen, the exergy and energy flow can be negative. This negative does not indicate the direction of flow, rather, the direction of flow is taken in the same direction as the mass flow.

The entropy and enthalpy values obtained by EES for the cold fluid, H_2O were verified by making use of the enthalpy and entropy values in Flownex®. For the hot fluid, CO_2, the values of Flownex® and EES did not match and was investigated further.

The enthalpy was determined for different states in EES. (A state refers to a set of values, where one is the temperature and one is the pressure.) The two enthalpy values were then

subtracted to obtain a difference - called a delta. Then the same two states were used and enthalpy values determined in Flownex®. Once again the enthalpy values were subtracted and a delta obtained. Now, the two deltas from the different programs were compared.

This whole procedure was followed for other states and each time the deltas were compared. It was found that the deltas agreed except for minor errors. When the percentages of these errors were analysed, they were determined to be very small. Some further research was done and it was concluded that there are different models/ polynomials that can be used to find thermodynamic properties. It was assumed that the two programs made use of different models/ polynomials and this was the reason for some minor errors. When enthalpy and entropy equations are used, the difference/ delta between two points are considered. As discussed earlier, the deltas are mostly the same even when different models are used. Thus, as long as the deltas between states are similar, you can use any model.

4.4 Normal Model

The next issue is to identify the points in the system where exergy will be computed and the points where energy flow will be computed. As the staggered grid approach was used to set up a model, this is a straightforward decision. Exergy is computed for each control volume or main grid point. Energy flow is computed between control volumes. For the pipes this is at each secondary grid point. For the wall, the energy flow rate is simply the heat transfer rate, computed by (4.3).

Table 4.3 shows the energy characterisation of the heat exchanger without a fault, where 4.3a depicts the exergy at main grid points and input boundaries and Table 4.3b the energy flow at secondary grid points and heat transfer through the two control volumes of the wall. The boundary conditions for these values are found in Table 4.4.

Table 4.3: Energy characterisation of heat exchanger without a fault

(a) Exergy on main grid points

Parameter	Value	Unit
Exergy of $M_{H_{in}}$	247920	J/kg
Exergy of M_{H1}	235210	J/kg
Exergy of M_{H2}	234370	J/kg
Exergy of $M_{C_{in}}$	905	J/kg
Exergy of M_{C1}	1933	J/kg
Exergy of M_{C2}	12985	J/kg
Exergy of M_{W1}	1938	J/kg
Exergy of M_{W2}	632	J/kg

(b) Energy flow of the system

Parameter	Value	Unit
Energy flow of S_{H1}	14020	W
Energy flow of S_{H2}	-2101	W
Energy flow of S_{H3}	-16706	W
Energy transfer Wall 1	16121	W
Energy transfer Wall 2	14606	W
Energy flow of S_{C1}	-5575	W
Energy flow of S_{C2}	9030	W
Energy flow of S_{C3}	25151	W

Table 4.4: Boundary conditions for energy characterisation

Parameter	Value	Unit
Hot fluid inlet pressure	9000	kPa
Hot fluid inlet temperature	410	K
Hot fluid outlet pressure	8800	kPa
Cold fluid inlet pressure	286	kPa
Cold fluid inlet temperature	290	K
Cold fluid outlet pressure	277.08	kPa

From the results of Table 4.3 it is clear that the exergy on the hot fluid is far greater than the exergy on the cold fluid side. Concerning the hot fluid side, there is a decrease in the exergy from the inlet side to the outlet side whilst the cold fluid side shows an increase in exergy from the inlet side to the outlet side.

Furthermore, it is important to note that a type of node law is adhered to. This follows the same principles as Kirchhoff's current law. Each control volume is seen as a node. If the direction of the energy flow rate is indicated by the direction of mass flow and the direction of the heat transfer, where a value that flows into a node is added and a value that flows out of a node is subtracted, we see that the sum of each node is zero or very close to zero. Small variances can be present and are attributed to the precision of the EES database and round-off errors.

4.4.1 Verification of energy characterisation based on the normal model

The exergy of the hot fluid side was expected to be much larger than the exergy of the cold fluid side. This is reflected in Table 4.3. Additionally, it was assumed that for the normal case, there is perfect insulation. This is confirmed by the adherence of the node low. All exergy values are positive which makes sense. The temperatures and pressures of the wall, hot fluid and cold fluid are well above the reference temperature and pressure. Since the entropy and enthalpy of the reference state is used, a negative value would indicate a flaw in the calculations or the operating conditions.

4.5 Faults

In this section, the exergy and energy flows of the model with the three types of faults will be considered. Despite the fact that extra components have been added in the Flownex® models, no extra control volumes, main grid points or secondary grid points are added for energy characterisations. The boundary conditions for all the faults are the same as the previous section and given by Table 4.4.

4.5.1 Model with fluid leak

The energy characterisation for the model with a fluid leak is obtained by following the same procedure as for the normal model. Table 4.5 depicts the exergy and energy flow values for the fluid leak energy characterisation.

Table 4.5: Energy characterisation of heat exchanger with a fluid leak

(a) Exergy on main grid points

Parameter	Value	Unit
Exergy of $M_{H_{in}}$	247920	J/kg
Exergy of M_{H1}	235210	J/kg
Exergy of M_{H2}	234370	J/kg
Exergy of $M_{C_{in}}$	905	J/kg
Exergy of M_{C1}	1665	J/kg
Exergy of M_{C2}	13028	J/kg
Exergy of M_{W1}	1947	J/kg
Exergy of M_{W2}	587	J/kg

(b) Energy flow of the system

Parameter	Value	Unit
Energy flow of S_{H1}	14040	W
Energy flow of S_{H2}	-2075	W
Energy flow of S_{H3}	-17178	W
Energy transfer Wall 1	16114	W
Energy transfer Wall 2	15103	W
Energy flow of S_{C1}	-5317	W
Energy flow of S_{C2}	9038	W
Energy flow of S_{C3}	24033	W

Table 4.5a shows that the exergy for the hot fluid side remains the same as in the normal case, however the exergy on the cold fluid side and on the wall changes. Table 4.5b shows that the energy flow values are mostly similar to the normal case, yet, the node law is not adhered to on the cold side at control volumes M_{C1} and M_{C2}. Considering control volume M_{C1} with the energy flow rate of S_{C1} entering the node, energy flow rate of S_{C2} leaving the volume and energy transfer of Wall 1 entering the volume:

$$(-5317\text{W}) - (9038\text{W}) + (15103\text{W}) = 748\text{W}. \tag{4.4}$$

(The energy flow rate is subtracted if it flows out of the control volume and is added if it flows into the control volume. Figure 3.4 is used to obtain the direction.) It was expected that the value of M_{C1} is not zero because the fluid leak is on the cold side. From the calcualtion it can be seen that 748 W excapes through the leak.

4.5.2 Model with heat leakage

Table 4.6 depicts the exergy and energy flow values of the energy characterisation of the heat exchanger with a heat leakage.

Table 4.6: Energy characterisation of heat exchanger with a heat leakage

(a) Exergy on main grid points

Parameter	**Value**	**Unit**
Exergy of $M_{H_{in}}$	247920	J/kg
Exergy of M_{H1}	234130	J/kg
Exergy of M_{H2}	243670	J/kg
Exergy of $M_{C_{in}}$	905	J/kg
Exergy of M_{C1}	291	J/kg
Exergy of M_{C2}	9109	J/kg
Exergy of M_{W1}	1564	J/kg
Exergy of M_{W2}	199	J/kg

(b) Energy flow of the system

Parameter	**Value**	**Unit**
Energy flow of S_{H1}	14516	W
Energy flow of S_{H2}	-4148	W
Energy flow of S_{H3}	-22955	W
Energy transfer Wall 1	18664	W
Energy transfer Wall 2	18806	W
Energy flow of S_{C1}	-5583	W
Energy flow of S_{C2}	2211	W
Energy flow of S_{C3}	20875	W

Table 4.6b shows that the heat transfer in the case of a heat leakage is larger when compared to the normal case. Inspecting the node law at control volume M_{C1}:

$$(-5583\text{W}) + (18806\text{W}) - (2211\text{W}) = 11012\text{W} \tag{4.5}$$

,

which is a large deviation from zero. This is to be expected as there is a heat leakage at M_{C1}. At all other nodes, the node law is adhered to. When the exergy of the heat leakage case is looked at in Table 4.6a it can be seen that the exergy values on the wall are notably smaller than the normal case. The exergy on Wall 2 is 632 J/kg for the normal case, whilst it is only 199 J/kg for the heat leakage case.

4.5.3 Model with fouling

Table 4.7 depicts the exergy and energy flow values of the energy characterisation of the heat exchanger with fouling.

Table 4.7: Energy characterisation of heat exchanger with fouling

(a) Exergy on main grid points

Parameter	Value	Unit
Exergy of $M_{H_{in}}$	247920	J/kg
Exergy of M_{H1}	238270	J/kg
Exergy of M_{H2}	232530	J/kg
Exergy of $M_{C_{in}}$	905	J/kg
Exergy of M_{C1}	6498	J/kg
Exergy of M_{C2}	26158	J/kg
Exergy of M_{W1}	3751	J/kg
Exergy of M_{W2}	1231	J/kg

(b) Energy flow of the system

Parameter	Value	Unit
Energy flow of S_{H1}	13458	W
Energy flow of S_{H2}	2955	W
Energy flow of S_{H3}	-9663	W
Energy transfer Wall 1	10502	W
Energy transfer Wall 2	12678	W
Energy flow of S_{C1}	-3059	W
Energy flow of S_{C2}	9559	W
Energy flow of S_{C3}	20059	W

In the case of fouling, Table 4.7b, shows that the node law is adhered to in all control volumes. Concerning the heat transfer, it is smaller than in the normal case. When Table 4.7a is compared to 4.3a, which is the normal case, the exergy on the hot fluid side remains the same, although on the cold fluid side and in the wall, the exergy values are considerably higher.

4.5.4 Verification of fault models

Concerning verification of the fault models; the behaviour as can be seen in Tables 4.5 - 4.7 was foreseen. The node law is adhered to on the hot fluid side, as all the faults are induced on the cold fluid side. Also with the fouling model, the node law also applies. Energy flow does not escape to the environment. In all cases, the exergy on the hot fluid side is much larger than the exergy on the cold fluid side. This is expected as the faults induced are not large enough to bring about a system change that would lead to negative exergy.

4.6 Conclusion

In this chapter, it was shown that it is possible to extract energy characterisations from the model developed in the previous chapter. Before exergy and energy flow rate formulas could

be applied, entropy and enthalpy values had to be calculated. This was an issue and solved by making use of EES. Energy characterisations were obtained for the heat exchangers with and without faults. There is a decrease of exergy from the hot side to the cold side. The node law was adhered to in certain instances and in other not. The energy characterisations were deemed sensible for the faultless heat exchanger and for the three faults as the energy information varied for each case.

Chapter 5

Graph theoretic approach

This chapter is concerned with the graph theoretic approach that is chosen and applied to the energy characterisations of the heat exchanger. A linear graph framework is proposed which makes it possible to pack all of the data from the energy characterisations into linear graphs. Thereafter, a technique called attributed graph matching is applied to compare the linear graph containing energy information of the heat exchanger without a fault to the linear graphs containing energy information of the heat exchanger with faults. By using this method, a cost matrix is obtained as well as a parameter that can be described as the distance between the two graphs.

5.1 Linear graph

In order to realise the objective of this study; to create an energy visualisation of the heat exchanger by means of a graph-based approach, a graph form must first be chosen. A decision needs to be made on how the information from the energy characterisation will be organised in a linear graph. It was decided that the exergy of main grid points or boundaries should be the attributes of the nodes and that the energy flow rate should describe the attributes of the edges. The linear graph used will constitute six nodes and eight edges. The nodes with exergy as attribute that will be used include:

- Hot side inlet boundary with specific exergy attribute x_1.
- Hot side control volume M_{H1} with specific exergy attribute x_2.
- Hot side control volume M_{H2} with specific exergy attribute x_3.
- Cold side control volume M_{C2} with specific exergy attribute x_4.
- Cold side control volume M_{C1} with specific exergy attribute x_5.
- Cold side inlet boundary with specific exergy attribute x_6.

The edges with energy flow as attribute that will be used include:

- Hot side secondary grid point S_{H1} with energy flow rate attribute $\dot{q}_1$.
- Hot side secondary grid point S_{H2} with energy flow rate attribute $\dot{q}_2$.
- Hot side secondary grid point S_{H3} with energy flow rate attribute $\dot{q}_3$.
- Heat transfer of wall 1 with energy flow rate attribute $\dot{q}_4$.
- Heat transfer of wall 2 with energy flow rate attribute $\dot{q}_5$.
- Cold side secondary grid point S_{C3} with energy flow rate attribute $\dot{q}_6$.
- Cold side secondary grid point S_{C2} with energy flow rate attribute $\dot{q}_7$.
- Cold side secondary grid point S_{C1} with energy flow rate attribute $\dot{q}_8$.

Figure 5.1 depicts the configuration of the linear graph used as well as the direction of the links; which corresponds to the direction of the mass flow in the pipes.

Originally, the control volumes on the separation wall, M_{W1} and M_{W2}, were also chosen as nodes. However, the temperature on the nodes are not measured by physical sensors in the system. Furthermore, if too many nodes are chosen, there might be data redundancy, whilst if too little nodes are chosen important data might be lost. For the above reasons and by testing different configurations and error, only six nodes were identified to sufficiently represent the energy in the system.

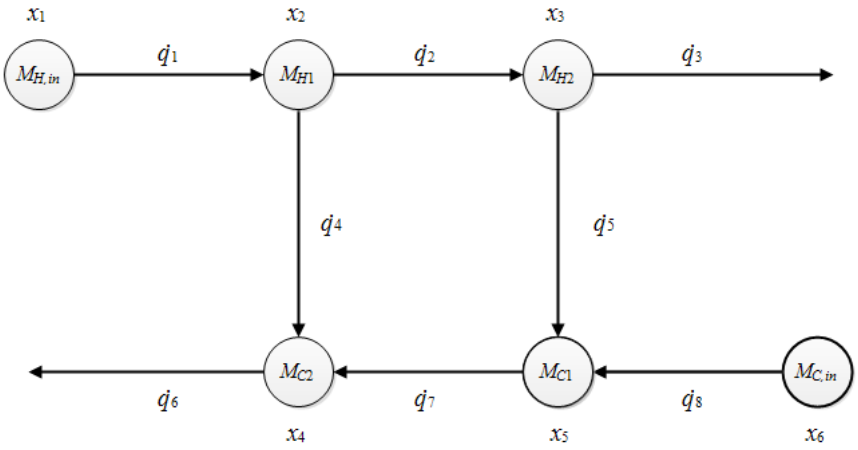

Figure 5.1: Linear Graph with energy information

5.2 Attributed graph matching

Graph matching is a technique that can be used to determine graph similarity. As discussed in Chapter 2, there multiple graph matching techniques that can be used. In this study it was decided to make use of the attributed graph matching technique of [57] that makes use of local descriptions.

With this technique, the local description of the attributed graph constitutes a node signature. A node signature matrix denoted by **N**, constitutes n vector rows, where n is the size of the graph, in other words, the number of nodes. Thus there is a vector row belonging to each node. The information for each row vector constitutes the attributes of the node, the degree of the node and the attributes of the incident edges. These vectors are then packed into a matrix called the node signature matrix. A node signature matrix is formed for both the original graph and the graph that will be compared to the original graph.

The next step is to compare the two graphs by comparing each vector in the original node signature matrix with every vector in the comparison node matrix. This comparison is achieved by making use of the Heterogeneous Euclidean Overlap Metric (HEOM) which can be used for both numeric and symbolic attributes [57]. In this study, only numeric attributes are present. Using the HEOM norm and the node signature matrices of the two linear graphs, a cost matrix is calculated. The element (i,j) in the cost matrix describes the distance between the ith row vector of the original graph node signature matrix and the jth row vector of the comparison

graph node signature matrix. Lastly a distance formula is defined that calculates the distance between two graphs by making use of the Hungarian method [57].

To demonstrate the graph matching technique and further details thereof, the following sections demonstrate how the techniques are applied to two attributed graphs. These linear graphs are obtained from the energy characterisations of the heat exchanger models by making use of the procedure described in section 5.1. A linear graph of the heat exchanger without a fault is used for the original graph and a linear graph of the heat exchanger with a fluid leak is used as the comparison graph. The energy information that will be used as the attributes for the nodes and the edges of the linear graphs are given in Tables 5.1 and 5.2. Table 5.1 contains the node attributes of the two graphs (basically the exergy information) and Table 5.2 contains the edge attribute for the two graphs (basically the energy flow rates).

Table 5.1: Node attributes

Parameter	**Original graph**	**Comaprison Graph**	**Unit**
x_1	247920	247920	J/kg
x_2	235210	235230	J/kg
x_3	234370	234470	J/kg
x_4	12985	13028	J/kg
x_5	1933	1665	J/kg
x_6	905	905	J/kg

Table 5.2: Edge attributes

Parameter	**Original graph**	**Comaprison Graph**	**Unit**
$\dot{q}_1$	14020.35	14039.50	W
$\dot{q}_2$	-2100.81	-2074.65	W
$\dot{q}_3$	-16706.33	-17177.87	W
$\dot{q}_4$	16121.16	16114.15	W
$\dot{q}_5$	14605.52	15103.22	W
$\dot{q}_6$	25150.93	24032.79	W
$\dot{q}_7$	9029.50	9038.01	W
$\dot{q}_8$	-5574.79	-5316.49	W

5.2.1 Node signature procedure

Now that the linear graphs have been identified and the attributes defined for each node and edge, the next step is to create a node signature matrix for each linear graph. This is done by creating a vector for every node. The vector is ordered as follows:

- The node attribute.
- The order of the node. (Number of edges incident on the node.)
- The attributes of the edges incident on the node, taking into account the directions of the arrows of Figure 5.1.
  - If edge direction is away from the node, multiply with 1.
  - If edge direction is into the node, multiply with -1.

Thus **N** = [columns with node attributes, column with order of each node, columns with node attributes]. The node signature matrix, $\mathbf{N}_O$, for the original graph is given by (5.1).

$$\mathbf{N}_O = \begin{bmatrix} 247920 & 1 & 14020.35 & 0 & 0 \\ 235210 & 3 & -14020.35 & -2100.81 & 16121.16 \\ 234370 & 3 & 2100.81 & -16706.33 & 14605.52 \\ 12985 & 3 & -16121.16 & 25150.93 & -9029.50 \\ 1933 & 3 & -14605.52 & 9029.50 & 5574.79 \\ 905 & 1 & -5574.79 & 0 & 0 \end{bmatrix} \tag{5.1}$$

The signature node matrix for the original graph has six rows, as there are six nodes. Also, the direction of mass-flow or heat transfer has been taken into account, so that the last three entries in each row sum up to zero. However, this is not applicable for the two boundary nodes.

The node signature matrix, $\mathbf{N}_F$, for the comparison graph is given by (5.2).

$$\mathbf{N}_F = \begin{bmatrix} 247920 & 1 & 14039.50 & 0 & 0 \\ 235230 & 3 & -14039.50 & -2074.65 & 16114.15 \\ 234470 & 3 & 2074.65 & -17177.87 & 15103.22 \\ 13028 & 3 & -16114.15 & 24032.79 & -9038.01 \\ 1665 & 3 & -15103.22 & 9038.01 & 5316.49 \\ 905 & 1 & -5316.49 & 0 & 0 \end{bmatrix} \tag{5.2}$$

The signature node matrix for the comparison graph has six rows, as there are six nodes. The last three entries in each row do not sum to zero for each row, the reason being that energy flow rate is lost through the fluid leak.

5.2.2 Procedure to obtain cost matrix

Following the acquisition of the signature node matrices, the HEOM norm is applied to obtain a cost matrix that describes the difference between the two graphs. Each row of the original matrix is compared to every row of the comparison matrix. In other words, a norm is obtained by taking the first row of the original matrix and the first row in the comparison matrix. Then a norm is obtained by taking the first row in the original matrix and the second row in the comparison matrix. This continues until there are six norms for the first row of the original matrix. Then the procedure is repeated for the second row of the original matrix, once again until there are six norms. When the procedure is finished, there are 36 norms which fit into a 6x6 matrix, where the element (*i,j*) is the HEOM norm of the *i*th row of the original matrix with the *j*th row of the comparison matrix.

Each norm is calculated using

$$HEOM(i,j) = \sqrt{\sum_{a=1}^{k} \delta(\mathrm{N}_{O_{ia}}, \mathrm{N}_{F_{ja}})}, \tag{5.3}$$

where $\mathrm{N}_{O_{ia}}$ refers to the (*i,a*) entry in the original matrix, $\mathrm{N}_{F_{ja}}$ refers to the (*j,a*) entry in the comparison matrix, k is the length of the row, a is the ath column vector and the function δ is given by

$$\delta(\mathrm{N}_{O_{ia}}, \mathrm{N}_{F_{ja}}) = \frac{|\mathrm{N}_{O_{ia}} - \mathrm{N}_{F_{ja}}|}{range_a}, \tag{5.4}$$

where $N_{F_{ja}}$ and $N_{F_{ja}}$ are the matrix entries as described above and $range_a$ is given by

$$range_a = |(ia + (0.05 \times ia)) - (ia - (0.05 \times ia))|. \tag{5.5}$$

If row one of the original node signature matrix is compared with row one of the comparison node signature matrix, the norm is given by

$$HEOM(1,1) = \sqrt{0 + 0 + 0.00018656 + 0 + 0} = 0.0137 \tag{5.6}$$

and the cost matrix, **C**, with all the norms are given as:

$$\mathbf{C} = \begin{bmatrix} 0.0137 & 16247.1755 & 22873.2765 & 25676.0917 & 10485.7831 & 17.0144 \\ 25.4024 & 0.1254 & 72.6828 & 125.7370 & 54.3635 & 19.5503 \\ 58.9432 & 77.3334 & 0.4597 & 91.9975 & 84.1596 & 39.8779 \\ 182.5634 & 173.7479 & 173.8362 & 0.4459 & 19.2319 & 19.3884 \\ 1272.8131 & 1207.1275 & 1203.5106 & 65.2591 & 1.5010 & 17.6968 \\ 2729.6743 & 16452.1924 & 23018.4181 & 25676.4373 & 10485.7751 & 0.4633 \end{bmatrix}. \tag{5.7}$$

5.2.3 Distance between graphs

A formula to calculate the distance between two attributed graphs is proposed in [57] as:

$$D(g_i, g_j) = \frac{\hat{M}}{|M|} + ||g_i| - |g_j||, \tag{5.8}$$

where $|g_i|$ is the number of nodes of graph i, $|M|$ is the number of matching operators and $\hat{M}$ is the sum of matching operating costs. The matching operators are obtained by applying the Hungarian algorithm to the cost matrix.

The Hungarian algorithm is an optimization method that solves an assignment problem [58]. When the algorithm is applied to the cost matrix, **C**, a permutation matrix, **P**, is obtained, this is given by equation 5.9.

$$\mathbf{P} = \begin{bmatrix} 1 & 0 & 0 & 0 & 0 & 0 \\ 0 & 1 & 0 & 0 & 0 & 0 \\ 0 & 0 & 1 & 0 & 0 & 0 \\ 0 & 0 & 0 & 1 & 0 & 0 \\ 0 & 0 & 0 & 0 & 1 & 0 \\ 0 & 0 & 0 & 0 & 0 & 1 \end{bmatrix} \tag{5.9}$$

The number of ones in **P** are the number of matching operators, whilst the sum of matching operators is given by summing specific values in the cost matrix. The specific values of the cost matrix that must be summed are the entry positions that correspond to the entry positions of the ones in the permutation matrix. In this example, the ones lie on the diagonal of the permutation matrix and thus it is the diagonal entries of the cost matrix that must be summed.

Thus for the two graphs that were used, a linear graph of the energy of the heat exchanger under normal conditions and a linear graph of the energy of the heat exchanger with a fluid leak, the distance is given by applying (5.8):

$$D = \frac{0.0137 + 0.1254 + 0.4597 + 0.4459 + 1.5010 + 0.4633}{6} + |6 - 6| = 0.5015. \tag{5.10}$$

The numerator is given by the sum of the diagonal entries of the cost matrix, **C**, as the ones of the permutation matrix, **P**, are on the diagonal.

5.3 Verification

The process does not need to be verified as it is based on the work done by [57] where it has been applied on a pattern recognition problem with success. For verification of the MATLAB® functions and programs used to obtain the cost matrix and distance, some of the matrix entries were checked by hand.

5.4 Conclusion

The notion to pack the energy characterisations of the heat exchanger with and without faults into linear graphs with six nodes and eight edges was successful. The output of the attributed graph matching technique is a cost matrix - describing similarities between two graphs by looking at subsections of the graphs - and a distance parameter - a scalar value that describes the magnitude with which two graphs differ. It should be noted that the cost matrix is in the form of a matrix, allowing the use of various matrix techniques and procedures. The cost matrix will form the base of the energy visualisation of the next chapter.

Chapter 6

Energy Visualisation

This chapter is concerned with the energy visualisation of the heat exchanger obtained by computing eigenvalues. A visualisation of the heat exchanger under normal conditions is proposed as an energy reference signature, to which the visualisations of the fault conditions can be compared. Cases with various boundary conditions are discussed along with cases where the degree of the faults are varied. Lastly a fault identification procedure is proposed that makes use of the energy visualisations to identify which type of fault has occurred. The distance parameter of the previous chapter will be used throughout to aid with comparisons.

6.1 Eigenvalues as visualisation tool

In linear algebra, the eigenvalues of a matrix are computed for various reasons. For a matrix $\mathbf{A}$, the Euclidean norm is given as the square root of the largest eigenvalue of $\mathbf{A}^*\mathbf{A}$ ($\mathbf{A}^*$ is the conjugate transpose of $\mathbf{A}$). Eigenvalues are used to diagonalize a matrix and to find the Jordan norm. With the Jordan norm, one can calculate the powers of a matrix and can apply functions to matrices. The eigenvalues of a matrix can also be used to determine if a matrix is singular or non-singular [59].

In control theory, the eigenvalues of the $\mathbf{A}$ matrix are computed to determine if the system

is controllable, observable and stable. Thus, the eigenvalues supply the characteristics of the system. One can also find the eigenvalues present in the transfer function of the system as the poles [60].

The above include only some of the most popular reasons that eigenvalues are used and in truth it reveals that eigenvalues are in essence a way to see into the heart of a matrix and define some of the characteristics. As a result, the eigenvalues of the different fault cost matrices (explained in the previous chapter) will be determined and visualised. In order to achieve visualisation, the eigenvalues will be plotted on the complex plane; since eigenvalues can either be real or complex.

The MATLAB® function "*eig()*" is used to determine the eigenvalues of the cost matrices and they are plotted on the complex plane by making use of the "*plot()*" function. The eigenvalues are determined from the cost matrix, which is a description of how the energy information in two graphs differ. As a result, the eigenvalues contain energy information. In fact, the eigenvalues determined by this procedure will be known as an energy visualisation. The following sections will explain how the energy visualisation of the different faults are used to find a procedure that identifies which fault has occurred.

6.2 Reference energy signature

In the previous chapter, attributed graph matching was applied to the node signature matrices of the different models and cost matrices were obtained. The next challenge is to visualise how the cost matrices change for each of the faults and if the visualisations are unique. This will be done by making use of eigenvalues. However, a baseline that will be used for comparison purposes is required.

A baseline is created for a specific set of boundary conditions by matching the graph to itself with the attributed graph matching procedure of the previous chapter. The resulting cost matrix is a matrix with zeros on the diagonal, nevertheless, the eigenvalues of this cost matrix are not zero. The eigenvalues of this baseline are called the reference energy signature and is generated for every set of boundary conditions.

6.3 Visualisation

In this section the energy visualisations for the three types of faults and energy reference signature for a specific set of boundaries will be shown. This specific set is called Boundary set I and the conditions are given in Table 6.1.

Table 6.1: Boundary conditions: Boundary set I

Parameter	Value	Unit
Hot fluid inlet pressure	8000	kPa
Hot fluid inlet temperature	396	K
Hot fluid outlet pressure	7800	kPa
Cold fluid inlet pressure	286	kPa
Cold fluid inlet temperature	302	K
Cold fluid outlet pressure	277.08	kPa

The reference energy signature for set I is depicted in Figure 6.1. Note that there are six eigenvalues as the cost matrix is a 6x6 matrix. There is one positive real eigenvalue, three negative real eigenvalues and a pair of complex conjugate eigenvalues. The eigenvalues are given in 6.2.

Table 6.2: Reference signature eigenvalues: Boundary set I

Real	Imaginary
-3472	-
-566	+ 43
-566	- 43
-51	-
-18	-
4672	-

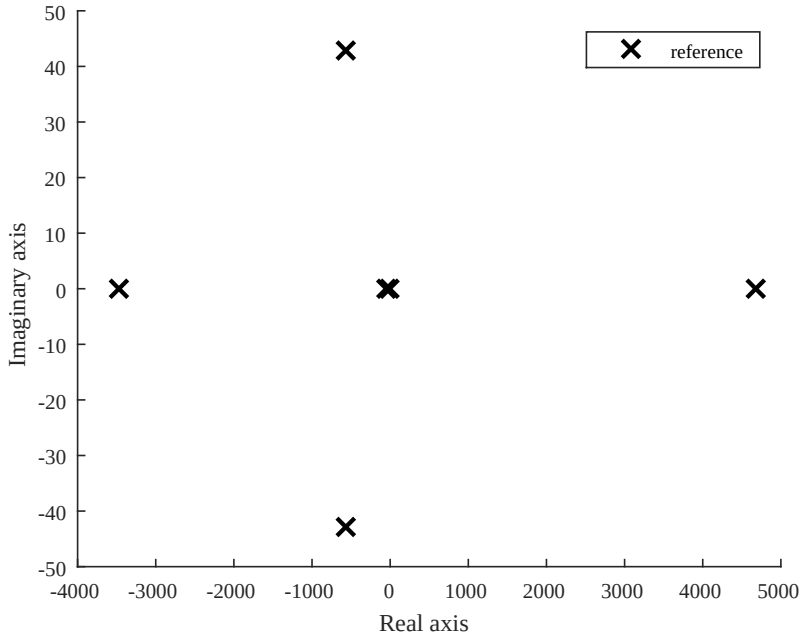

Figure 6.1: Energy reference signature: Boundary set I

6.3.1 Visualisation of a leak

Figure 6.2 depicts the energy reference signature along with the energy visualisation of a fluid leak. A quick clarification is introduced that is needed for the rest of the chapter: a set of corresponding eigenvalues refer to the eigenvalue of the energy visualisation that is closest to an eigenvalue of the energy reference signature. For example the two real positive eigenvalues, with values of about 4671, 873 and 4696.040, in Figure 6.2 are corresponding.

Figure 6.2 shows that the energy visualisation of the leak has six eigenvalues, denoted by the circles, of which one is positive and real, three are negative real and two are complex. This is the same as for the energy reference which also has one real positive eigenvalue, three real negative eigenvalues and two complex eigenvalues. Observe that the values of each corresponding eigenvalue differ from the reference eigenvalues. For the real eigenvalues, the difference is relatively small (the circles and x's are almost on top of each other) whilst for the complex eigenvalues, the differences are significant. The eigenvalues for the for the energy characterisation of the fluid leak is given by Table 6.3.

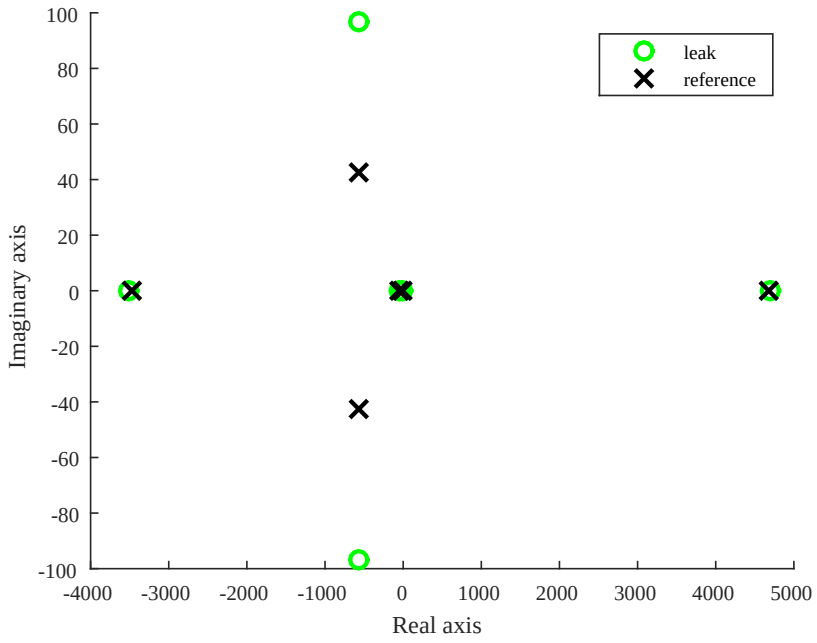

Figure 6.2: Energy visualisation of a leak (Boundary set I)

Table 6.3: Fluid leak eigenvalues (Boundary set I)

Real	**Imaginary**
-3506	-
-559	+ 97
-559	- 97
-51	-
-18	-
4696	-

6.3.2 Visualisation of a heat leakage

Figure 6.3 depicts the energy reference signature along with the energy visualisation of a heat leakage. Observe that there are six eigenvalues, of which one is positive and real, three are negative real and two are complex. Concerning the most negative real eigenvalue, it varies significantly from the most negative real value of the reference signature. The complex values also differ significantly from the reference complex values. On the other hand, the other

three real eigenvalues differ little form the corresponding reference signature values. The eigenvalues for the energy characterisation of the heat leakage is given by Table 6.4.

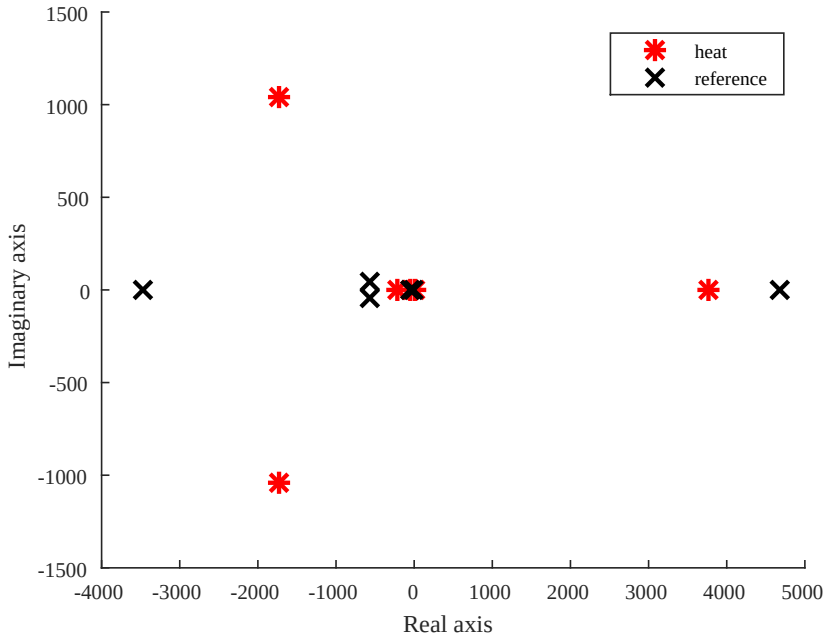

Figure 6.3: Energy visualisation of a heat leakage (Boundary set I)

Table 6.4: Heat Leakage eigenvalues (Boundary set I)

Real	**Imaginary**
-216	-
-1735	+ 1037
-1735	- 1037
-55	-
19	-
3771	-

6.3.3 Visualisation of fouling

Figure 6.4 depicts the energy reference signature along with the energy visualisation of the heat exchanger with fouling. Observe that there are six eigenvalues, of which one is positive and real, one is negative real and four are complex. Thus, an extra pair of complex eigenvalues are present. When the largest and smallest real eigenvalues of the reference and the heat leakage

visualisation are compared, a significant difference is noticed. The eigenvalues for the energy characterisation of fouling is given by Table 6.5.

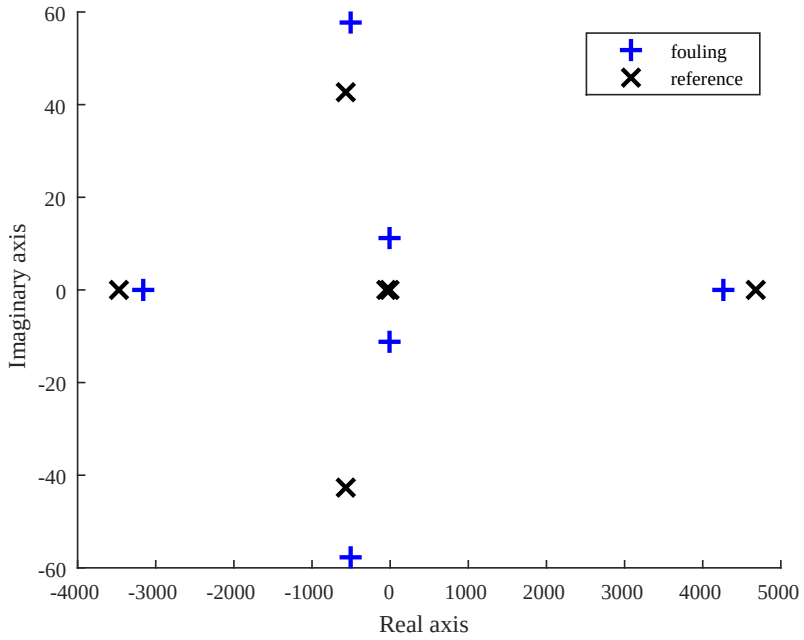

Figure 6.4: Energy visualisation of fouling (Boundary set I)

Table 6.5: Fouling eigenvalues (Boundary set I)

Real	**Imaginary**
-3152	-
-507	+ 58
-507	- 58
-13	+ 11
-13	- 11
4260	-

6.3.4 Visualisation of all faults

Figure 6.5 depicts the energy reference signature along with the energy visualisations of all three faults. It can be noted that the corresponding eigenvalues vary the least in the case of a leak and vary the most in the case of a heat leakage. The distance parameters (as described in the previous chapter) for the different faults are given as:

- Leak: 0.4493
- Heat leakage: 8.2223
- Fouling: 11.1395

The distance parameters reflect the variation in the corresponding eigenvalues for each of the visualisations. Importantly Figure 6.5 reveals that the energy visualisation is different for each of the faults. Consequently, it confirms that the attributed graph matching technique along with the way in which the energy visualisations were defined, are successful in visualising the different faults uniquely.

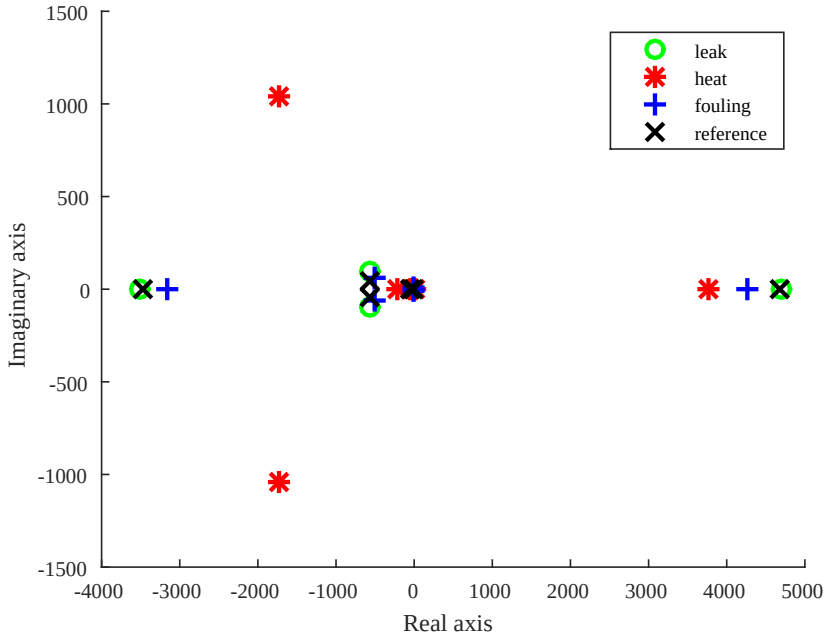

Figure 6.5: Energy visualisation - Case 1 (Boundary set I)

The specific boundary conditions set and fault parameters from section 3.5 used to obtain Figure 6.5 is called Case 1. Other cases will now be looked at.

6.4 Different cases and scenarios

In the previous section the energy visualisations of a specific set of boundaries called Boundary set I were considered. The faults that were considered were based on the fault parameters

as explained in section 3.5. Nevertheless, a heat exchanger can be operated with different boundary conditions and the degree of the faults can also vary. For instance, the hot fluid can be at a higher temperature or the leak in the cold fluid pipe can either be very small or large. Consequently, more cases need to be considered, cases where other boundary conditions are applied and cases where the degrees of the faults are adjusted. The aforementioned cases are described and the respective energy visualisation considered in the following subsections.

6.4.1 Adjustment of fault degrees

Two cases are considered; in Case 2, the degree of the fault is greater than in Case 1, in Case 3, the degree of the fault is smaller than in Case 1. Both Cases 2 and 3 have the same boundary conditions as Case 1, Boundary set I, given by Table 6.1. The fault parameters for Cases 1, 2 and 3 are given in Table 6.6. Figures 6.6 and 6.7 depict the energy visualisations for Cases 2 and 3 respectively.

The energy visualisations of Cases 2 and 3 are very similar to that of Case 1. In all cases, the energy reference signatures have one positive real eigenvalue, three negative real eigenvalues and a pair of complex conjugate eigenvalues. In all three cases, the visualisations of the fluid leak have one positive real eigenvalue, three negative real eigenvalues and a pair of complex conjugate eigenvalues. The energy visualisations of the heat leakage are also similar with two positive real eigenvalue, two negative real eigenvalues and a pair of complex conjugate eigenvalues. For fouling the visualisations differ, in Case 1, there was two sets of complex eigenvalues. In Cases 2 and 3, there are only one set of complex eigenvalues. The eigenvalues for Cases 2 and 3 are given in Tables 6.7 and 6.8 respectively.

Table 6.6: Fault parameters

Parameter	**Case 1**	**Case 2**	**Case 3**	**Unit**
Leak pipe diameter	0.001	0.002	0.0005	m
Heat leakage area	.803	1	0.5	m^2
Fouling K-forward factor	30	50	10	N/A

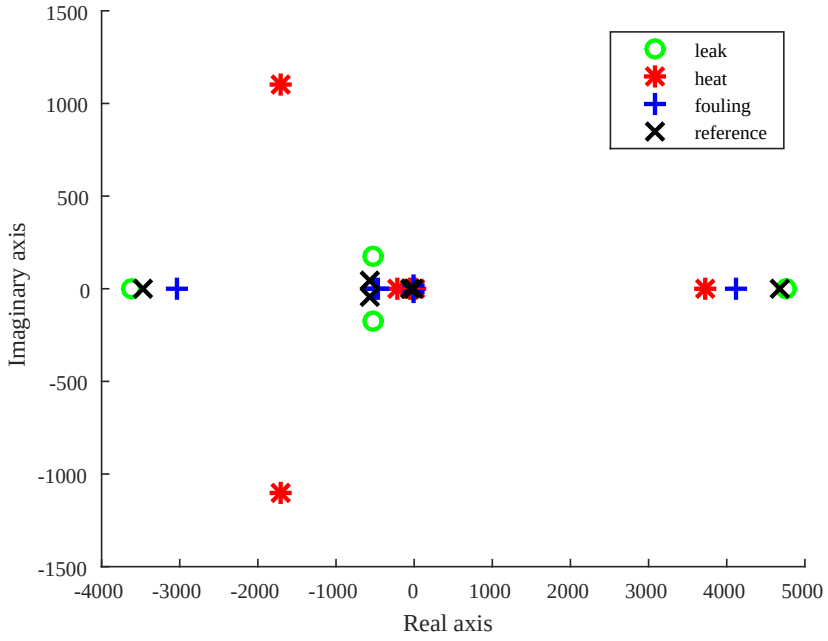

Figure 6.6: Energy visualisation: Case 2 (Boundary set I)

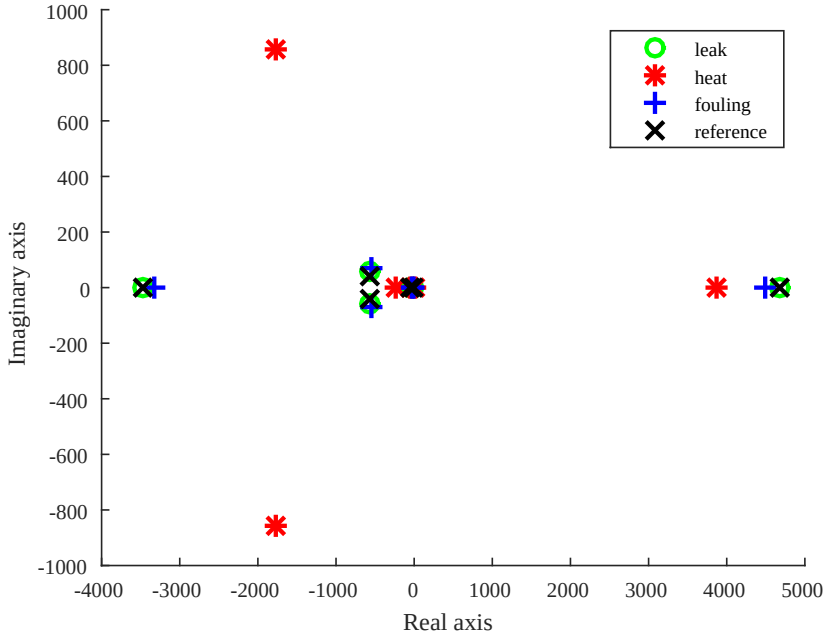

Figure 6.7: Energy visualisation: Case 3 (Boundary set I)

Table 6.7: Eigenvalues: Case 2 (Boundary set I)

Reference	**Fluid leak**	**Heat leak**	**Fouling**
-3471	-3607	-209	-3030
-566 + 43i	-534 + 179	-1719 + 1099i	-7 + 14
-566 - 44i	-534 - 179i	-1719 - 1099i	-7 -14i
-50	-50	-55	-515
-18	-19	21	-468
4672	4757	3733	4117

Table 6.8: Eigenvalues: Case 3 (Boundary Set I)

Reference	**Fluid leak**	**Heat leak**	**Fouling**
-3471	-3480	-235	-3329
-566 + 43i	-564 + 61i	-1778 + 854i	-538 + 70i
-566 - 43i	-564 + 61i	-1778 + 854i	-538 + 70i
-50	-51	-53	-31
-18	-18	14	-17
4672	4678	3874	4483

Table 6.9 gives the distance parameters for Cases 1, 2 and 3. When Figures 6.5, 6.6 and 6.7 are compared, it can be observed that all the forms of the energy visualisations remain the same. In comparison with Case 1, observe that the corresponding eigenvalues vary less in Case 3, whilst they vary more in Case 2. In brief, it appears that the energy visualisations reflect the degree of the faults. Similarly, the degree of the faults is reflected in the distance parameters of Table 6.9.

Table 6.9: Distance parameters for Cases 1,2 and 3

Parameter	**Case 1**	**Case 2**	**Case 3**
Leak	0.449	2.298	0.108
Heat leakage	8.222	8.578	7.289
Fouling	11.140	14.946	5.147

6.4.2 Adjustment of boundary conditions

Table 6.10 supplies the boundary conditions that are called Boundary Set II and used in Case 4. Compared to Case 1; all the boundary conditions of both the hot fluid side and the cold fluid side have been adjusted. The fault parameters remain the same as in section 3.5.

Using Boundary Set II as given by Table 6.10, the whole procedure is repeated. Parameter values obtained are from the Flownex® model and used to calculate energy values which are packed into linear graphs, then attributed graph matching is applied and the eigenvalues of the respective cost matrices are visualised. Figure 6.8 displays the energy visualisation for Case 4. The distance parameters are given as:

- Leak: 1.950
- Heat leakage: 11.162
- Fouling: 13.984

Table 6.10: Boundary conditions: Boundary Set II

Parameter	Value	Unit
Hot fluid inlet pressure	8400	[kPa]
Hot fluid inlet temperature	402	[K]
Hot fluid outlet pressure	8200	[kPa]
Cold fluid inlet pressure	287	[kPa]
Cold fluid inlet temperature	303	[K]
Cold fluid outlet pressure	278.08	[kPa]

When Figure 6.8 is compared to Figure 6.5 a significant difference is noted for the energy reference signature. All the eigenvalues are real. In this case the energy visualisations for the two fluid leak also contains only real eigenvalues. The energy visualisation for heat leakage contains only one set of complex eigenvalues and two positive real values, which is the same as in Case 1. Concerning the energy visualisation for fouling, in there is one set of complex eigenvalues which differs from Case 1, which has two sets. When comparing the distance

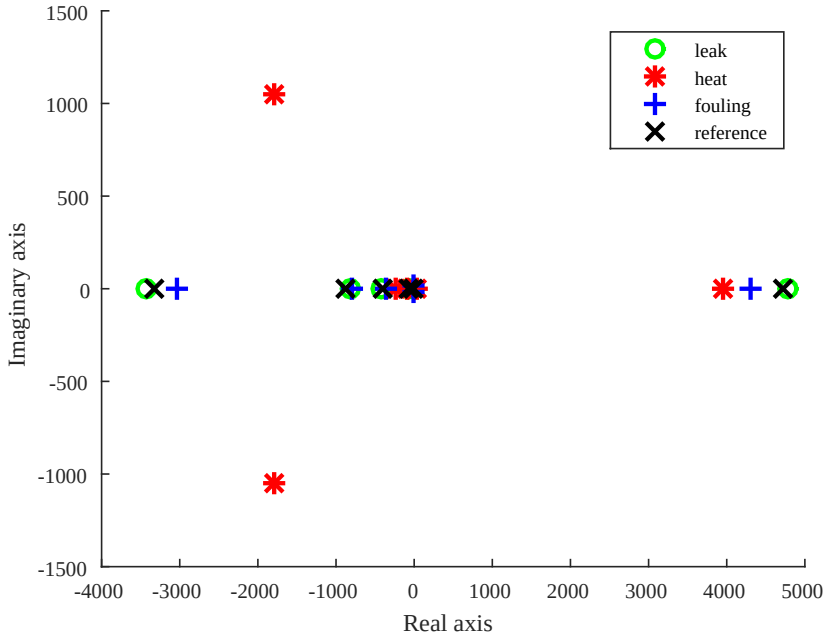

Figure 6.8: Energy visualisation - Case 4 (Boundary Set II)

parameters, the parameters are larger for Case 4. This was expected as both the heat leakage and fouling fault visualisations contain at least one set of complex values whilst the reference signature does not.

Table 6.11: Eigenvalues - Case 4 (Boundary Set II)

Reference	**Fluid leak**	**Heat leakage**	**Fouling**
-3335	-3439	-232	-3039
-886	-819	-1798 + 1053i	-15 + 13i
-398	-422	-1798 - 1053i	-15 - 13i
-15	-15	-82	-789
-75	-75	23	-353
4710	4780	3954	4295

6.5 Fault identification procedure

At this point the challenge is to define a procedure that can identify which fault has occurred when only the data of the energy reference signature and one energy visualisation are available. In this instance the type of fault of the energy visualisation is not known. A procedure was developed by making use of cases 1-4 and other cases (different boundary conditions and different fault magnitudes) not discussed in the previous sections, but can be found in Appendix B. These include cases where all boundary condition parameters were adjusted and cases where only one boundary condition parameter was adjusted. The procedure makes use of ”if” logic and each fault is unique. The procedure is described in Table 6.12. The procedure makes use of the energy reference signature and the energy visualisation concerned. Each ”if” rule is given a number that will be used later.

Table 6.12: Identification Procedure

	If condition	**Fault if true**
1	Energy-visualisation has two positive real eigenvalues.	Heat leakage
2	The most negative real eigenvalue of the energy visualisation is more negative than the most negative value of the reference signature **AND** the most positive real eigenvalue of the energy visualisation is more positive than the most positive value of the reference signature.	Fluid leak
3	None of the above criteria are met. (Can also be: The most negative real eigenvalue of the energy visualisation is less negative than the most negative value of the reference signature **AND** the most positive real eigenvalue of the energy visualisation is less positive than the most positive value of the reference signature)	Fouling

6.6 Verification

In order to verify the use of eigenvalues to create an energy visualisation two factors are considered. The first is that each energy visualisation is unique which is necessary since the faults are unique and the energy characterisation is different for every fault. The second is the

fact that the degree to which each set of corresponding eigenvalues differ, corresponds with the magnitude of the distance parameter. In turn the distance parameter can be trusted since it has been applied in [57] with success.

Concerning the verification of the identification procedure, it was tested on different cases (where the fault was not disclosed beforehand). These cases include both cases that were used to create the procedure as well as cases that were not used. Table 6.13 gives the "if" number of the identification procedure (of Table 6.12) that was used to identify each of the three faults for ten different cases. The case numbers are identified by C1, C2 etc. The boundary conditions, fault parameters and eigenvalues for Cases 5 - 10 are found in Appendix B.

Table 6.13: Identification of faults according to procedure

	C1	**C2**	**C3**	**C4**	**C5**	**C6**	**C7**	**C8**	**C9**	**C10**
Fluid leak	2	2	2	2	2	2	2	2	2	2
Heat leakage	1	1	1	1	1	1	1	1	1	1
Fouling	3	3	3	3	3	3	3	3	3	3

6.7 Conclusion

This chapter has revealed that it was sensible to calculate and plot the eigenvalues of the cost matrix - obtained by graph matching and based on energy data - as a means to energy visualisation. The procedure that was developed for fault identification was tested on various cases and was successful in identifying the three different types of faults. The results of this chapter confirm that graph matching is a valid approach. Similarly, the use of energy data to identify faults is sensible and provides a comprehensive method to pack information into a graph that is representative of all the domains in system.

Chapter 7

Conclusion

In this chapter conclusions will be drawn from the results of previous chapters. The usefulness, shortcomings and problems of the issues addressed in the study will be discussed. The chapter continues with recommendations for possible future work.

7.1 Conclusions

The counter-flow, single phase heat exchanger model in this study is based on the gas cooler of an operating CO_2 heat pump test bench. The choice was made to use a pre-existing validated Flownex® model. This increased the validity of the results and allowed energy visualisation and graph matching to be the primary focus points of the study.

A side-by-side simplified two-dimensional approach towards modelling the counter-flow heat exchanger was followed. Six control volumes were identified. The argument exists that six volumes might not be enough to fully represent a system which is normally modelled in a distributive manner. Nevertheless, an objective of the study was the fault diagnosis of a heat exchanger. In fault diagnosis, the reduction of system data is of value. Sensor availability is another reason for choosing a smaller number of control volumes.

Three types of faults were introduced in the Flownex model®. The faults were introduced one at a time and only on the cold fluid pipe. The system response to the faults was as excepted.

In order to achieve a visualisation, energy information had to be extracted from the model. The choice to make use of exergy and energy flow rates presented some difficulties at first. Even though Flownex® had access to enthalpy and entropy values of some points, only temperature, pressure and mass flow data are available from sensors. The problem was solved by making use of EES. The next challenge was the reference state that had to be used. At first, the reference state was not chosen and used correctly - this led to data that did not make sense. The problem was solved by discussing the issue with chemical and mechanical engineers with knowledge of thermodynamics. When the correct reference state was chosen and implemented correctly; the data made sense and a node law was adhered to as explained in Chapter 4. The fact that enthalpy values could be negative was another confusing aspect. Later it was realised that the negative sign did not indicate direction but has everything to do with the reference state chosen. In the end, by applying the energy equations, energy information was obtainable for each control volume, boundary condition, secondary point and heat transfer point. Energy information could also be extracted for the three different faults and the values could be compared.

The decision was made to use two boundary conditions and four control volumes as the nodes of the attributed linear graph. If the control volumes on the separation wall were used, the energy heat transfer rates would be duplicated in the graph. For the reason of data redundancy, the wall's control volumes were left out. Two boundary conditions were selected as nodes, so that the energy visualisation obtained would be directly dependent of the boundary conditions used.

The literature study showed that graph matching as used in pattern recognition would be the most appropriate technique to use. Moreover, one of the simplest techniques in the pattern recognition field was identified. A simpler technique would allow the focus to remain on the energy in the system on how it changed when different faults were introduced. In order to understand the technique better, it was applied on two simple electric circuit configurations constituting two resistors, an inductor and a capacitor. This was not discussed in this study.

The motivation for applying the technique by Jouili et al [57] was their use of a cost matrix and distance parameter. In addition to the permutation matrix, the cost matrix and distance

parameter would supply more information of how the graphs corresponded. This proved to be a valid decision. The energy graphs were similar and the permutation matrices were the same for most of the cases. On the other hand, the cost matrices differed and provided more information.

In creating an energy visualisation, it was decided to make use of a baseline. The baseline was named the energy reference signature and was associated with a certain set of boundary conditions. The idea was that any one of the faults could be compared to the reference signature. For various reasons, eigenvalues were chosen to achieve visualisation. Two significant reasons include; eigenvalues give insight into the characteristics of a matrix and eigenvalues can be represented in two-dimensions. For the sake of comprehending the visualisation results, it was decided that visualisation had to be kept at three dimensions or lower.

The procedure developed for fault detection has been tested and was successful in detecting a fluid leak, heat leakage and fouling. However, the procedure can only identify an individual fault and not simultaneous faults.

7.2 Recommendations and future work

The model used in the study is very basic and only the steady state response of the heat exchanger was considered. In future work, a more complex model could be used and the transient response of the heat exchanger should also be taken into account.

It was decided that the attributed linear graph constituted six nodes and eight edges. This decision was based on careful considerations regarding data redundancy, information reduction and the model used. Further investigation into the graph size could be done in order to determine how the optimum configuration links to the model used and how the configuration affects data redundancy and reduction.

The use of eigenvalues for energy visualisation proved to be of great significance. Future work could look at the use of eigenvectors in energy visualisation. Based on the success of eigenvalues, the forecast is that more insight would be gained into the energy change in the system and also that the detection procedure could benefit from the inclusion of eigenvectors.

Only a single fault can be detected by the procedure. Future work could investigate the effects of simultaneous faults and if the graph matching approach is still successful in identifying faults.

In this study, only verification was of concern. It would be beneficial to investigate the validity of the specific approach taken. Furthermore, the credibility of the approach would be enhanced if a Monte Carlo analysis is performed.

Lastly, it is proposed that using graph matching as a means to energy visualisation should be evaluated on other systems or processes. It would be interesting to see how the approach translates and what aspects would need the most consideration.

7.3 Closure

The objective of developing energy visualisations for a counter-flow heat exchanger, by making use of graph matching was achieved. Additionally, the energy visualisations are sensitive to faults. Energy characterisations were extracted from a Flownex® heat exchanger model. This was done for the model without a fault and with faults. The energy characterisations were packed into attributed linear graphs of size 6. The technique of graph matching was applied to the graphs and two-dimensional energy visualisations achieved by calculating eigenvalues. A procedure was developed for the identification of faults which proved to be successful.

Bibliography

[1] International Energy Agency, *Key world energy statistics*, 2016th ed., Paris, 2016. [Online]. Available: www.iea.org

[2] D. Jeltsema and J. M. Scherpen, "Multidomain modeling of nonlinear networks and systems: Energy- and power-based perspectives," *IEEE Control Systems Magazine*, vol. 29, no. August, pp. 28–59, 2009.

[3] Y. A. Çengel, *Heat Transfer: A Practical Approach*, ser. McGraw-Hill series in mechanical engineering. McGraw-Hill, 2003.

[4] T. L. Bergman, A. S. Lavine, F. P. Incropera, and D. P. DeWitt, "Fundamentals of heat and mass transfer, 2011," *USA: John Wiley & Sons. ISBN*, vol. 13, pp. 470–978, 2015.

[5] B. A. Qureshi and S. M. Zubair, "Predicting the impact of heat exchanger fouling in power systems," *Energy*, vol. 107, pp. 595–602, 2016.

[6] H. A. Almohamad, "A polynomial transform for matching pairs of weighted graphs," *Applied mathematical modelling*, vol. 15, no. 4, pp. 216–222, 1991.

[7] R. Sinha, V.-C. Liang, C. J. Paredis, and P. K. Khosla, "Modeling and Simulation Methods for Design of Engineering Systems," *Journal of computing and information science in engineering*, vol. 1, no. 1, pp. 84–91, 2001.

[8] N. Deo, *Graph Theory with Applications to Engineering and Computer Science*. Prentice-Hall of India, 1984.

[9] G. Van Schoor, K. R. Uren, M. A. van Wyk, P. A. van Vuuren, and P. Carel, "An energy perspective on modelling, supervision, and control of large-scale industrial systems: Survey and framework," *IFAC World Congress*, pp. 6692–6703, 2014.

[10] W. M. Haddad and S. G. Nersesov, *Stability and control of large-scale dynamical systems: A Vector Dissipative Systems Approach*. Princeton University Press, 2011.

[11] J. W. Chinneck and M. Chandrashekar, "Models of large-scale industrial energy systems I. Simulation," *Energy*, vol. 9, no. 1, pp. 21–34, 1984.

[12] H.-J. Marais, G. van Schoor, and K. R. Uren, "An Energy-based approach to condition monitoring of industrial processes," *IFAC-PapersOnLine*, vol. 48, no. 21, pp. 772–777, 2015.

[13] S. Persin and B. Tovornik, "Real-time implementation of fault diagnosis to a heat exchanger," *Control engineering practice*, vol. 13, no. 8, pp. 1061–1069, 2005.

[14] K. R. Uren and G. Van Schoor, "Energy-based visualisation of a counter-flow heat exchanger for the purpose of fault identification," *Procedings of the 11th IFAC Symposium on Dynamics and Control of Process Systems Including Biosystems DYCOPS*, pp. 19–24, 2016.

[15] K. J. Reinschke, "Multivariable control: a graph theoretic approach," *Lecture Notes in Control and Information Sciences*, 1988.

[16] C. Schmitke and J. McPhee, "Using linear graph theory and the principle of orthogonality to model multibody, multi-domain systems," *Advanced Engineering Informatics*, 2008.

[17] E. I. Varga, K. M. Hangos, and F. Szigeti, "Controllability and observability of heat exchanger networks in the time-varying parameter case," *Control Engineering Practice*, vol. 3, no. 10, pp. 1409–1419, 1995.

[18] A. Leitold, K. M. Hangos, and Z. Tuza, "Structure simplification of dynamic process models," *Journal of Process Control*, vol. 12, no. 1, pp. 69–83, 2002.

[19] F. Tu, K. R. Pattipati, S. Deb, and V. N. Malepati, "Computationally efficient algorithms for multiple fault diagnosis in large graph-based systems," *IEEE Transactions on Systems, Man, and Cybernetics-Part A: Systems and Humans*, vol. 33, no. 1, pp. 73–85, 2003.

[20] S. Chessa and P. Santi, "Comparison-based system-level fault diagnosis in ad hoc networks," in *Reliable distributed systems, 2001. Proceedings. 20th IEEE Symposium on*. IEEE, 2001, pp. 257–266.

[21] Q. Wang, M. Zeng, T. Ma, X. Du, and J. Yang, "Recent development and application of several high-efficiency surface heat exchangers for energy conversion and utilization," *Applied Energy*, vol. 135, no. 748-777, 2014.

[22] F. P. Incropera, A. S. Lavine, T. L. Bergman, and D. P. DeWitt, *Principles of heat and mass transfer*, 7th ed. Wiley, 2013.

[23] B. Gao, Q. Bi, and M. Gui, "Experimental performance comparison of shell-side heat transfer for shell-and-tube heat exchangers with different helical baffles," *Heat Transfer Engineering*, no. just-accepted, pp. 1–52, 2016.

[24] M. M. Abu-Khader, "Plate heat exchangers: recent advances," *Renewable and sustainable energy reviews*, vol. 16, no. 4, pp. 1883–1891, 2012.

[25] R. K. Shah and D. P. Sekulic, *Fundamentals of heat exchanger design*. John Wiley & Sons, 2003.

[26] Y. A. Cengel, A. J. Ghajar, and H. Ma, *Heat and Mass Transfer: Fundamentals & Applications, 4e*. McGraw-Hill, 2011.

[27] K. Thulukkanam, *Heat exchanger design handbook*. CRC Press, 2013.

[28] P. Gupta and M. D. Atrey, "Performance evaluation of counter flow heat exchangers considering the effect of heat in leak and longitudinal conduction for low-temperature applications," *Cryogenics*, vol. 40, no. 7, pp. 469–474, 2000.

[29] B. Dawoud, E.-H. Amer, and D.-M. Gross, "Experimental investigation of an adsorptive thermal energy storage," *International journal of energy research*, vol. 31, no. 2, pp. 135–147, 2007.

[30] S. Ding, *Model-based fault diagnosis techniques: design schemes, algorithms, and tools*. Springer Science & Business Media, 2008.

[31] W. Chen, "Fault detection and isolation in nonlinear systems," Ph.D. dissertation, Universität Duisburg-Essen, Fakultät für Ingenieurwissenschaften Elektrotechnik und Informationstechnik Automatisierungstechnik und komplexe Systeme, 2012.

[32] I. Dincer and Y. A. Cengel, "Energy, entropy and exergy concepts and their roles in thermal engineering," *Entropy*, vol. 3, no. 3, pp. 116–149, 2001.

[33] M. Kanouglu, Y. A. Çengel, and I. Dinçer, *Efficiency evaluation of energy systems*. Springer Science & Business Media, 2012.

[34] C. Borgnakke and R. E. Sonntag, *Fundamentals of thermodynamics*, 8th ed. Wiley, 2009.

[35] B. J. van Wyk and M. A. van Wyk, "Kronecker product graph matching," *Pattern Recognition*, vol. 36, no. 9, pp. 2019–2030, 2003.

[36] K.-S. Fu, "A step towards unification of syntactic and statistical pattern recognition." *IEEE transactions on pattern analysis and machine intelligence*, vol. 8, no. 3, p. 398, 1986.

[37] W.-H. Tsai and K.-S. Fu, "Error-correcting isomorphisms of attributed relational graphs for pattern analysis," *IEEE Transactions on systems, man, and cybernetics*, vol. 9, no. 12, pp. 757–768, 1979.

[38] A. K. C. Wong, M. You, and S. C. Chan, "An algorithm for graph optimal monomorphism," *IEEE Transactions on Systems, Man, and Cybernetics*, vol. 20, no. 3, pp. 628–638, 1990.

[39] S. Umeyama, "An eigendecomposition approach to weighted graph matching problems," *IEEE transactions on pattern analysis and machine intelligence*, vol. 10, no. 5, pp. 695–703, 1988.

[40] S. Peleg, "A new probabilistic relaxation scheme," *IEEE Transactions on Pattern Analysis and Machine Intelligence*, no. 4, pp. 362–369, 1980.

[41] R. A. Hummel and S. W. Zucker, "On the foundations of relaxation labeling processes," *IEEE Transactions on Pattern Analysis and Machine Intelligence*, no. 3, pp. 267–287, 1983.

[42] S. Z. Li, "Matching: invariant to translations, rotations and scale changes," *Pattern Recognition*, vol. 25, no. 6, pp. 583–594, 1992.

[43] S. Gold and A. Rangarajan, "A graduated assignment algorithm for graph matching," *IEEE Transactions on pattern analysis and machine intelligence*, vol. 18, no. 4, pp. 377–388, 1996.

[44] P. D. Simić, "Constrained nets for graph matching and other quadratic assignment problems," *Neural Computation*, vol. 3, no. 2, pp. 268–281, 1991.

[45] T.-W. Chen and W.-C. Lin, "A neural network approach to CSG-based 3-D object recognition," *IEEE Transactions on Pattern Analysis and Machine Intelligence*, vol. 16, no. 7, pp. 719–726, 1994.

[46] P. N. Suganthan, E. K. Teoh, and D. P. Mital, "Pattern recognition by graph matching using the potts MFT neural networks," *Pattern Recognition*, vol. 28, no. 7, pp. 997–1009, 1995.

[47] H. A. Almohamad and S. O. Duffuaa, "A linear programming approach for the weighted graph matching problem," *IEEE Transactions on pattern analysis and machine intelligence*, vol. 15, no. 5, pp. 522–525, 1993.

[48] M. A. Van Wyk and J. Clark, "An algorithm for approximate least-squares attributed graph matching," *Problems in applied mathematics and computational intelligence*, pp. 67–72, 2000.

[49] M. A. Van Wyk, T. S. Durrani, and B. J. van Wyk, "A RKHS interpolator-based graph matching algorithm," *IEEE Transactions on Pattern Analysis and Machine Intelligence*, vol. 24, no. 7, pp. 988–995, jul 2002.

[50] B. J. Van Wyk and M. A. Van Wyk, "The spherical approximation graph matching algorithm," in *Proc. International Workshop on Multidisciplinary Design Optimization*, 2000, pp. 280–288.

[51] O. D. Faugeras and K. E. Price, "Semantic description of aerial images using stochastic labeling," *IEEE Transactions on Pattern Analysis and Machine Intelligence*, no. 6, pp. 633–642, 1981.

[52] M. A. Van Wyk, B. J. Van Wyk, and T. J. Van Rensburg, "Approximate least-squares attributed graph matching via bayesian inference," in *Fourteenth Annual Symposium of the Pattern Recognition Association of South Africa*. Citeseer, 2003, p. 119.

[53] M-Tech Industrial, "Flownex Simulation Environment." [Online]. Available: http://www.flownex.com/

[54] S. B. Smuts, "An energy-based representation of a counter flow single phase heat exchanger," Masters dissertation, North-West University, 2015.

[55] S. Patankar, *Numerical heat transfer and fluid flow*. CRC press, 1980.

[56] Y. A. Cengel and M. A. Boles, *Thermodynamics: an engineering approach*, 5th ed. McGraw-Hill, 2006.

[57] S. Jouili, I. Mili, and S. Tabbone, "Attributed graph matching using local descriptions," in *International Conference on Advanced Concepts for Intelligent Vision Systems*. Springer, 2009, pp. 89–99.

[58] H. W. Kuhn, "The Hungarian method for the assignment problem," *Naval Research Logistics (NRL)*, vol. 52, no. 1, pp. 7–21, 2005.

[59] C. D. Meyer, *Matrix analysis and applied linear algebra*. Siam, 2000, vol. 2.

[60] C. Heij, A. C. M. Ran, and F. van Schagen, *Introduction to mathematical systems theory: linear systems, identification and control*. Springer Science & Business Media, 2006.

Appendix A

EES Macro files

Figure A.1 depicts the EES Macro file that was called by MATLAB® to calculate the enthalpy and entropy values of a fluid and store it in a temporary file. The specific material's name and three different temperatures and pressures are input for the file and are supplied by MATLAB®.

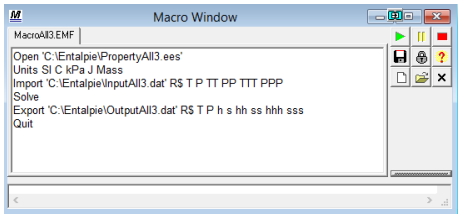

Figure A.1: Macro file to obtain enthalpy and entropy of CO_2 and H_2O

Figure A.2 depicts the EES Macro file that was called by MATLAB® to calculate the enthalpy and entropy values of a solid and store it in a temporary file. The specific material's name and two different temperatures and pressures are input for the file and are supplied by MATLAB®.

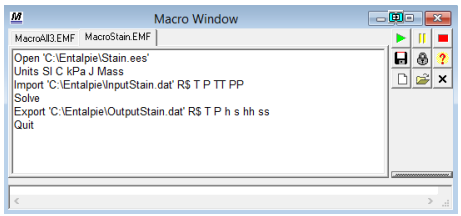

Figure A.2: Macro file to obtain enthalpy and entropy of AISI 304 stainless steel

Appendix B

Data cases for energy visualisation

The boundary conditions sets, fault parameters and eigenvalues for Cases 5-10 are given in the following sections.

B.1 Case 5

Table B.1: Boundary conditions for Case 5

Parameter	Value	Unit
Hot fluid inlet pressure	9000	[kPa]
Hot fluid inlet temperature	410	[K]
Hot fluid outlet pressure	8800	[kPa]
Cold fluid inlet pressure	286	[kPa]
Cold fluid inlet temperature	302	[K]
Cold fluid outlet pressure	277.08	[kPa]

Table B.2: Fault parameters for Case 5

Parameter	Value	Unit
Leak pipe diameter	0.001	m
Heat leakage area	.803	m^2
Fouling K-forward factor	30	N/A

Table B.3: Eigenvalues: Case 5

Reference	Fluid leak	Heat leak	Fouling
-3305	-3353	-307	-2926
-1107	-1078	-1961 + 912i	-1018
-394	-399	-1961 - 912i	-323
-170	-171	-184	-34
-8	-9	35	-22
4983	5013	4485	4475

B.2 Case 6

Table B.4: Boundary conditions for Case 6

Parameter	Value	Unit
Hot fluid inlet pressure	8800	[kPa]
Hot fluid inlet temperature	410	[K]
Hot fluid outlet pressure	8600	[kPa]
Cold fluid inlet pressure	286	[kPa]
Cold fluid inlet temperature	300	[K]
Cold fluid outlet pressure	277.08	[kPa]

Table B.5: Fault parameters for Case 6

Parameter	Value	Unit
Leak pipe diameter	0.001	m
Heat leakage area	.803	m^2
Fouling K-forward factor	30	N/A

Table B.6: Eigenvalues: Case 6

Reference	Fluid leak	Heat leak	Fouling
-3051	-3066	-1204	-2734
-1272 + 1491i	-1289 + 1520i	-1835 + 1124i	-1147 + 1393i
-1272 -1491i	-1289 - 1520i	-1835 + 1124i	-1147 -1393i
-133 + 49i	-136 + 45i	-171	-61 + 53i
-133 - 49i	-136 -45i	145	-61 - 53i
5859	5918	4977	5299

B.3 Case 7

Table B.7: Boundary conditions for Case 7

Parameter	Value	Unit
Hot fluid inlet pressure	8800	[kPa]
Hot fluid inlet temperature	410	[K]
Hot fluid outlet pressure	8600	[kPa]
Cold fluid inlet pressure	286	[kPa]
Cold fluid inlet temperature	302	[K]
Cold fluid outlet pressure	277.08	[kPa]

Table B.8: Fault parameters for Case 7

Parameter	Value	Unit
Leak pipe diameter	0.001	m
Heat leakage area	.803	m^2
Fouling K-forward factor	30	N/A

Table B.9: Eigenvalues: Case 7

Reference	Fluid leak	Heat leak	Fouling
-3454	-3506	-356	-3074
-1046	-448	-2043 + 687i	-934
-444	-448	-2043 - 687i	-357
-231	-233	-245	-64
-3	-4	42	–11
5178	5210	4779	4635

B.4 Case 8

Table B.10: Boundary conditions for Case 8

Parameter	Value	Unit
Hot fluid inlet pressure	8300	[kPa]
Hot fluid inlet temperature	400	[K]
Hot fluid outlet pressure	8200	[kPa]
Cold fluid inlet pressure	288	[kPa]
Cold fluid inlet temperature	300	[K]
Cold fluid outlet pressure	280	[kPa]

Table B.11: Fault parameters for Case 8

Parameter	Value	Unit
Leak pipe diameter	0.0015	m
Heat leakage area	.75	m^2
Fouling K-forward factor	25	N/A

Table B.12: Eigenvalues: Case 8

Reference	Fluid leak	Heat leak	Fouling
-3489	-3535	-1410	-3296
-751 + 1131i	-763 + 1186i	-1291 + 1103i	-974 +1049i
-751 - 1131i	-763 - 1186i	-1291 - 1103i	-974 -1049i
-93	-156	-6	-82
-46	-40	88	-25
5129	5213	3946	4799

B.5 Case 9

Table B.13: Boundary conditions for Case 9

Parameter	Value	Unit
Hot fluid inlet pressure	8300	[kPa]
Hot fluid inlet temperature	302	[K]
Hot fluid outlet pressure	8200	[kPa]
Cold fluid inlet pressure	286	[kPa]
Cold fluid inlet temperature	302	[K]
Cold fluid outlet pressure	277.08	[kPa]

Table B.14: Fault parameters for Case 9

Parameter	Value	Unit
Leak pipe diameter	0.0015	m
Heat leakage area	.75	m^2
Fouling K-forward factor	25	N/A

Table B.15: Eigenvalues: Case 9

Reference	Fluid leak	Heat leak	Fouling
-3803	-3883	-226	-3523
-467 + 288i	-452 + 311i	-1727 + 825i	-424 + 271i
-467 - 288i	-452 - 311i	-1727 - 825i	-424 - 271i
-21	-28	-30	-13 +7i
-27	-21	11	-13 - 7i
4785	4840	3735	4441

B.6 Case 10

Table B.16: Boundary conditions for Case 10

Parameter	Value	Unit
Hot fluid inlet pressure	7500	[kPa]
Hot fluid inlet temperature	398	[K]
Hot fluid outlet pressure	7300	[kPa]
Cold fluid inlet pressure	286	[kPa]
Cold fluid inlet temperature	302	[K]
Cold fluid outlet pressure	277.08	[kPa]

Table B.17: Fault parameters for Case 10

Parameter	Value	Unit
Leak pipe diameter	0.0008	m
Heat leakage area	1.2	m^2
Fouling K-forward factor	15	N/A

Table B.18: Eigenvalues: Case 10

Reference	Fluid leak	Heat leak	Fouling
-3602	-3626	-255	-3420
-547 + 165i	-543 +177i	-1736 + 988i	-506 + 170i
-547 - 165i	-543 - 177i	-1736 - 988i	-506 - 170i
-10	-89	-92	-48i
-88	-10	36	-8
4795	4813	3849	4547